

# A game-theoretic mechanism for aggregation and dispersal of interacting populations

Russ deForest\* and Andrew Belmonte†

Department of Mathematics  
Pennsylvania State University,  
University Park, PA 16802 USA

July 13, 2021

## Abstract

We adapt a fitness function from evolutionary game theory as a mechanism for aggregation and dispersal in a partial differential equation (PDE) model of two interacting populations, described by density functions  $u$  and  $v$ . We consider a spatial model where individuals migrate up local fitness gradients, seeking out locations where their given traits are more advantageous. The resulting system of fitness gradient equations is a degenerate system having spatially structured, smooth, steady state solutions characterized by constant fitness throughout the domain. When populations are viewed as predator and prey, our model captures prey aggregation behavior consistent with Hamilton's selfish herd hypothesis. We also present weak steady state solutions in 1d that are continuous but in general not smooth everywhere, with an associated fitness that is discontinuous, piecewise constant. We give numerical examples of solutions that evolve toward such weak steady states. We also give an example of a spatial Lotka–Volterra model, where a fitness gradient flux creates instabilities that lead to spatially structured steady states. Our results also suggest that when fitness has some dependence on local interactions, a fitness-based dispersal mechanism may act to create spatial variation across a habitat.

---

\*email: russ.f.deforest@gmail.com, corresponding author

†email: andrew.belmonte@gmail.com

**keywords:** dispersal, aggregation, fitness gradient, degenerate diffusion, quasilinear pde, cross-diffusive instability, evolutionary game dynamics, migration.

**MSC: Primary 92D25; Secondary 35K65**

## 1 Introduction

An interesting problem in ecology is understanding the aggregation behavior seen in some prey species in the presence of predators. In some settings, such as bait balls of mackerel in the open ocean, aggregation provides an easy target for large predators even as the behavior diffuses the risk to each individual [31]. Thus, aggregation can be viewed as a cooperative behavior.

In his 1971 paper, *Geometry of the Selfish Herd*, Hamilton hypothesized that the aggregation behavior in a prey species could arise from the selection pressure of predators [21]. Under the *selfish herd hypothesis* each animal seeks to minimize its individual domain of danger in the presence of a predator that may appear at a random location. Hamilton proposed a nearest neighbor rule; by moving in the direction of the nearest neighbor, prey animals reduce their individual domains of danger. There are two interesting shortcomings of this assumption, noted by Hamilton in his original paper. First, the rule tends to produce small isolated clusters instead of large aggregations. Another is that an animal may temporarily increase its domain of danger in its approach to its nearest neighbor. A variety of movement rules have followed. A review paper by Morrell and James summarizes movement rules that have been considered and analyzes their success in capturing aggregation behavior in various settings [27].

In this paper we adapt a fitness function from evolutionary game theory as a mechanism for aggregation in a predator-prey model. The model seeks to capture transitory dynamics of the interacting populations as each locates itself on the landscape relative to the other. We have in mind aggregation phenomena such as bait balls where species of prey fish densely pack themselves together in the presence of predators [31].

Our modeling assumptions will be shown to encode assumptions of Hamilton's *selfish herd hypothesis*; prey tend to aggregate so as to maximize their population density relative to the population of predators and the predators follow. Steady states are characterized by the condition where the relative

frequency of the two populations is constant. Our model can also be viewed as capturing the spatial dynamics of a public goods type game, where both a cooperating and defecting population each increase their fitness by locating themselves in regions where the relative frequency of cooperators is higher.

As is standard in evolutionary games, the fitness in our model depends on the relative frequency of each population [22]. However, we are not modeling selection dynamics among competing traits or strategies. Instead we model the spatial dynamics as each population tends to move up its local fitness gradient. The resulting model is a degenerate quasilinear system of partial differential equations which we refer to as a *fitness gradient flux system* of partial differential equations (PDE). The most interesting feature of the model is the presence of a negative density-dependent diffusion coefficient for the prey population. Naturally, this is the feature in the model that gives rise to the aggregation phenomenon. The prey aggregation is moderated by the predator population which “chases” the prey. We show that a perturbation of the model yields a *normally parabolic* system, having smooth solutions. Thus, despite the negative self-diffusion coefficient, the degeneracy should be viewed as a limiting case of a well-behaved system. We also note that the mechanism for aggregation differs from that used in the Keller-Segel chemotaxis model where aggregation follows a chemical gradient and is moderated by self-diffusion [11, 23].

We present results on steady state solutions and on a linearization around these steady states. We then discuss a Lotka–Volterra predator-prey model spatially extended via the fitness-gradient flux.

## 1.1 The model

We consider here a spatial model of two populations without selection, driven by migration only in the direction of increasing fitness, resulting from a *fitness gradient flux*. This flux arises naturally from the effort of individuals within each population as they seek out, locally, positions of greater advantage. The dynamics of the population densities can be modeled by the following partial differential equations (PDEs) in a bounded domain  $\Omega \subset \mathbb{R}^n$ ,

with a no-flux boundary condition and strictly positive initial conditions

$$\begin{cases} \partial_t u = -\beta_1 \nabla \cdot (u \nabla f_1), & \text{in } \Omega \times (0, T), \\ \partial_t v = -\beta_2 \nabla \cdot (v \nabla f_2), & \text{in } \Omega \times (0, T), \\ \nu \cdot (u \nabla f_1) = 0, \quad \nu \cdot (v \nabla f_2) = 0, & \text{on } \partial\Omega \times (0, T), \\ u(\mathbf{x}, 0) = u_0(\mathbf{x}) > 0, & \text{in } \Omega, \\ v(\mathbf{x}, 0) = v_0(\mathbf{x}) > 0, & \text{in } \Omega, \end{cases} \quad (1.1)$$

where  $f_i$  describe the fitness for each population, the  $\beta_i$  are constants determining each population's sensitivity to its fitness gradient, and  $\nu$  is the outer unit normal to  $\partial\Omega$ . These equations, first presented in [15], describe population migration in the direction of increasing fitness. The resulting system can be viewed as a generalized diffusion system, where there are cross-diffusion effects (see Section 2).

It is interesting to contrast a steady state solution of (1.1) with an ideal free distribution. In an ideal free distribution a population is allocated to the available habitat in an optimal way. Fitness depends on local environmental conditions and is assumed to be a decreasing function of the local population density. Constant fitness is a characteristic of ideal free distributions, since if fitness were not a constant function of space, some individuals could relocate to more favorable habitat, improving their fitness [19, 14, 12].

As we show below in Section 5, for strictly positive steady state solutions of (1.1) the fitness functions  $f_i$  are constant throughout  $\Omega$ . However, our results differ from an ideal free distribution in several ways. In our model, an individual's fitness is the expected value of an interaction with another individual occupying the same local area and depends only on the ratio of the local population densities, consistent with an evolutionary game. As such, there are many possible steady states giving the same constant values for the fitness functions,  $f_i$ . Thus while populations at a steady state are optimally distributed, there is no dependence on the background environmental conditions, which are assumed to be uniform throughout the domain. The spatial structure of a particular steady state instead results from variations in the ratio of population densities throughout the domain at some initial time. This suggests that when fitness has some dependence on intraspecies and interspecies interactions, fitness-based dispersal may act as a source of variation across a habitat.

In Section 3 we treat a simplified version of (1.1) on two nodes. We derive this equation from a continuum limit argument in Section 4. Our main results appear in Section 5, where we discuss steady state solutions, weak steady state solutions, and show that smooth steady state solutions are unstable. Numerical examples are discussed in Section 6. In the remainder of this section we provide some background on PDE models of interacting populations.

## 1.2 Background on PDE Population Models

Although the use of diffusion in a PDE model of population dynamics originated with Fisher [18, 5], Skellam is credited as the first systematic treatment of diffusion in modeling the spread of biological populations [37, 4, 30, 8]. He further suggested that such models must account for attractive and repulsive forces that arise from animal behavior [36]. Okubo extended Skellam’s work along these lines by allowing a transition probability in a biased random walk to depend either on local conditions at a present node, or conditions at neighboring nodes and at intermediate locations [29].

The first use of fitness-based migration in a PDE model of biological populations seems to be by Shigesada, Kawasaki, and Teramoto, whose work (now called the SKT model) formalized Morisita’s theory of environmental density [35]. This theory, based on Morisita’s experimental work with antlions and observations of other species, assumes that the suitability of a given habitat declines with an increase in population density and can be thought of as a precursor to the assumptions used in define an ideal free distribution [26, 32]. The SKT model includes “the attractive force which induces directed movements of individuals toward favorable places”, as well as random movements (diffusion) and a nonlinear dispersive force due to population pressure. Their model demonstrates that dispersal due to population pressure can reduce interspecific competition by leading competitors to segregate spatially.

More recently, Cosner and Cantrell have used a fitness gradient flux in dynamic models whose steady state solutions approximate ideal free distributions [12, 9]. These are reaction-advection-diffusion models where the advective term represents directed movement up a local fitness gradient. The fitness is defined to be a local rate of reproduction and is a decreasing

function of the local population density. The key result is that such a local dispersal mechanism can lead to an ideal free distribution. An extension to a two-species competition model has been used to show that a species adopting a fitness-based dispersal cannot be invaded by a competitor using only random dispersal [10].

A model of ideally-motivated competitors was investigated in [33], demonstrating conditions for coexistence, spatial segregation, and competitive exclusion. A more recent paper by Cosner gives a thorough review of the use of reaction-diffusion-advection models in studying both the effects and evolution of dispersal as well as providing background on relevant analytical techniques [13].

The Keller-Segel chemotaxis model is a well studied system modeling aggregation. See the review in [23]. More recent work in aggregation-diffusion equations has been focused degenerate on diffusion and on aggregation with nonlocal effects incorporated via convolution with a potential [6, 7]. An interesting model in [24] uses convolution with a smooth potential to regularize a density dependent backward heat equation.

### 1.3 Background on Normally Parabolic Reaction Diffusion Systems

Our main results concern a degenerate system of equations with a negative, density dependent self-diffusion coefficient for one of the populations. Strong solutions for an approximation to this system, regularized by additional diffusion terms were shown to exist in [41].

Under a different regularization, this system may also be viewed as a limiting case of a normally parabolic reaction diffusion system. The theory of quasilinear normally parabolic systems is developed in a series of papers by Amann [1, 3, 2]. Such systems feature spatial operators that are normally elliptic, but in general are not strongly elliptic and they capture the smoothing property associated with the heat equation. That is to say such operators are generators of analytic semigroups which can be used to represent solutions in an appropriate function space. We state here a general, local in time existence result due to Amann for normally parabolic reaction-diffusion systems having a no-flux boundary. In the sequel we show that a regularization of our model results in such a system. While in this model

we focus on accessible features of the degenerate system, we are interested in further study of normally parabolic reaction-diffusion systems that retain key features of the present model.

Let  $\Omega$  be an open, bounded, and connected domain in  $\mathbb{R}^n$  with  $C^2$  boundary  $\partial\Omega$ . We consider a system of PDEs acting on real-valued functions  $\mathbf{u} = (u_1, \dots, u_d)$  given by

$$\partial_t u_k = \nabla \cdot (b_{k1} \nabla u_1 + \dots + b_{kd} \nabla u_d) + f_k(\mathbf{u}), \quad \text{for } k = 1, \dots, d, \quad (1.2)$$

satisfying the no-flux boundary condition

$$\sum_{k=1}^d b_{kj} \nu \cdot \nabla u_j = 0, \quad (1.3)$$

where  $\nu$  is the outer unit normal to  $\Omega$ . Define

$$G =: \{\xi \in \mathbb{R}^d : \sigma(B(\xi)) \subset [\operatorname{Re} z > 0]\}.$$

We take the coefficient functions  $b_{kj}(\cdot)$  and the “reaction” functions  $f_k(\cdot)$  to be smooth maps from  $G$  to  $\mathbb{R}$ :

$$b_{kj} \in C^\infty(G), \quad f_k \in C^\infty(G). \quad (1.4)$$

*Remark.* The set  $G$  is open in  $\mathbb{R}^d$ . For the PDE we consider we will want

$$R_{\geq 0}^d = \{x \in \mathbb{R}^d : x_i \geq 0 \text{ for all } i\} \subset G,$$

or at least

$$R_{> 0}^d = \{x \in \mathbb{R}^d : x_i > 0 \text{ for all } i\} \subset G.$$

Expressing the spatial differential operator in (1.2) in the form

$$\mathcal{B}(\mathbf{u})\mathbf{u} = \nabla \cdot [B(\mathbf{u})\nabla\mathbf{u}],$$

and the boundary operator in (1.3) in the form

$$\mathcal{C}(\mathbf{u})\mathbf{u} = 0,$$

we can rewrite our PDE in the form

$$\begin{aligned} \partial_t \mathbf{u} &= \mathcal{B}(\mathbf{u})\mathbf{u} + \mathbf{f}(\mathbf{u}), \\ \mathcal{C}(\mathbf{u})\mathbf{u} &= 0 \end{aligned} \quad (1.5)$$

Finally, let  $V$  denote the space of  $\mathbb{R}^d$ -valued functions in  $W^{1,p}(\Omega)$  that take values in  $G$ :

$$V := \{ \mathbf{v} \in W^{1,p}(\Omega) : \mathbf{v}(\overline{\Omega}) \subset G \}.$$

We use the following local existence theorem [3, pg. 17].

**Theorem 1** (Amann Normally Parabolic Local Existence). *For any  $\mathbf{u}_0 \in V$ , the PDE given by*

$$\begin{cases} \partial_t \mathbf{u} = B(\mathbf{u})\mathbf{u} + \mathbf{f}(\mathbf{u}), & \text{in } \Omega \times (0, T), \\ C(\mathbf{u})\mathbf{u} = 0, & \text{on } \partial\Omega \times (0, T), \\ \mathbf{u}(\cdot, 0) = \mathbf{u}_0, & \text{on } \Omega, \end{cases} \quad (1.6)$$

*satisfying (assumptions above) has a unique maximal solution,*

$$\mathbf{u}(\cdot) \in C([0, t_f]) \cap C^\infty(\overline{\Omega} \times (0, t_f), \mathbb{R}^d). \quad (1.7)$$

*The map  $t \mapsto \mathbf{u}(t)$  defines a smooth semiflow on  $V$ , in the  $W^{1,p}(\Omega)$  sense. Furthermore, if  $\mathbf{u}(t)$  is a bounded orbit that is also bounded away from the boundary  $\partial V$  then  $\mathbf{u}(t)$  is relatively compact in  $V$  and for  $t > 0$  is also bounded in  $W^{2,p}(\Omega)$ .*

*Remark.* In general,  $t_f$  depends on the initial condition  $\mathbf{u}_0$ . If  $\mathbf{u}(t)$  remains bounded in  $W^{1,p}(\Omega)$  and bounded away from  $\partial V$  then we may take  $t_f = \infty$ ; existence is global.

## 2 Recasting the Model as a Generalized Diffusion System

Here we calculate fitness gradients based on fitness functions from an evolutionary game for two populations and recast (1.1) as a generalized degenerate diffusion system. We also demonstrate a regularizing perturbation that results in a normally parabolic quasilinear system.

We first consider the following system, first presented in [15], where we've denoted the fitness for  $u$  as  $f_1$ ; the fitness for  $v$  is denoted by  $f_2$ :

$$\begin{cases} \partial_t u = -\beta_1 \nabla \cdot (u \nabla f_1), & \text{in } \Omega \times (0, T) \\ \partial_t v = -\beta_2 \nabla \cdot (v \nabla f_2), & \text{in } \Omega \times (0, T), \end{cases} \quad (2.1)$$

The constants  $\beta_i$  denote each population's responsiveness or sensitivity to its individual fitness gradient. By letting  $\beta = \frac{\beta_2}{\beta_1}$  and rescaling time, we may re-write (2.1) as

$$\begin{cases} \partial_t u = -\nabla \cdot (u \nabla f_1), & \text{in } \Omega \times (0, T) \\ \partial_t v = -\beta \nabla \cdot (v \nabla f_2), & \text{in } \Omega \times (0, T), \end{cases} \quad (2.2)$$

Now let  $A$  denote a two strategy symmetric game matrix,

$$A = \begin{bmatrix} a_{11} & a_{12} \\ a_{21} & a_{22} \end{bmatrix}.$$

The fitness functions for  $u$  and  $v$  are

$$f_1(u, v) = \frac{a_{11}u + a_{12}v}{u + v}, \quad f_2(u, v) = \frac{a_{21}u + a_{22}v}{u + v}. \quad (2.3)$$

This definition of fitness, which we base on Taylor and Jonker [38], is standard in the evolutionary game literature (see also [39], [16], [17, Ch. 7],[22]).

This leads to

$$\begin{aligned} \nabla f_1(u, v) &= \frac{(a_{11} - a_{12})}{(u + v)^2} (v \nabla u - u \nabla v) \\ \nabla f_2(u, v) &= \frac{(a_{21} - a_{22})}{(u + v)^2} (v \nabla u - u \nabla v). \end{aligned} \quad (2.4)$$

Noting that the fitness gradients are proportional, we define a constant depending on the matrix  $A$ ,

$$\kappa_A = \frac{(a_{21} - a_{22})}{(a_{11} - a_{12})},$$

so that

$$\nabla f_2 = \kappa_A \nabla f_1.$$

As we have done in (1.1), we will usually denote the fitness function for  $u$  as  $f(u, v)$ . The corresponding fitness gradient for  $v$  is then

$$\kappa_A \nabla f.$$

By defining a parameter  $\gamma > 0$  such that

$$(1 + \gamma) = \kappa_A,$$

we arrive at the following PDE system.

$$\begin{cases} \partial_t u = -\nabla \cdot (u \nabla f), & \text{in } \Omega \times (0, T) \\ \partial_t v = -(1 + \gamma) \nabla \cdot (v \nabla f), & \text{in } \Omega \times (0, T), \\ \nu \cdot (u \nabla f) = \nu \cdot (v \nabla f) = 0, & \text{on } \partial\Omega \times (0, T), \\ u(x, 0) = u_0(x) > 0, & \text{in } \Omega, \\ v(x, 0) = v_0(x) > 0, & \text{in } \Omega. \end{cases} \quad (2.5)$$

We normalize the game matrix, making the assumption that  $a_{11} - a_{12} = 1$ ; we also assume that  $\gamma > 0$  which requires that  $a_{21} - a_{22} > 1$ . Thus  $v$  is more responsive to  $\nabla f$  than the population  $u$ .

*Remark.* This game dynamic is one where players of type  $u$  do best against their own type, while individuals of type  $v$  do better against type  $u$  than against others of their own type. This is the case in the classical prisoner's dilemma and hawk-dove games. As discussed in the introduction, a similar dynamic exists in predator-prey systems where prey aggregate and by so doing, reduce their individual risk of predation while predators benefit by locating themselves where prey is highly concentrated [21, 34, 40]. We are not considering Nash equilibria of the game given by  $A$ ; our interest here is only in how the game matrix  $A$ , though the parameter  $\gamma$ , affects the movement and distribution of the populations.

From (2.4) with  $a_{11} - a_{12} = 1$  we have

$$\begin{aligned} -u \nabla f &= \frac{1}{(u+v)^2} (-uv \nabla u + u^2 \nabla v) \\ -(1+\gamma) \nabla f &= \frac{(1+\gamma)}{(u+v)^2} (-v^2 \nabla v + uv \nabla v) \end{aligned}$$

It is sometimes convenient to express (2.5) in the vector form

$$\partial_t \mathbf{w} = \nabla \cdot (b(\mathbf{w}) \nabla \mathbf{w}), \quad (2.6)$$

where  $\mathbf{w} = (u, v)$  and  $\nabla \mathbf{w} = (\nabla u, \nabla v)$ , where  $B(\cdot)$  a matrix of density dependent diffusion coefficients with

$$B(u, v) = \frac{1}{(u+v)^2} \begin{bmatrix} -uv & u^2 \\ -(1+\gamma)v^2 & (1+\gamma)uv \end{bmatrix}. \quad (2.7)$$

*Remark.* It is now clear how our choice of fitness functions for the two populations encodes the assumption that both the prey population  $u$  and the predator population  $v$  tend toward regions where the population  $u$  has higher density. The term  $-uv\nabla u$  in the flux for  $u$  drives the prey aggregation, while the term  $u^2\nabla v$  indicates that prey are also seeking to move away from higher concentrations of the predators. Meanwhile the term  $-v^2\nabla v$  indicates the predators are chasing the prey, while the term  $uv\nabla v$  indicates some intraspecies competition among predators.

Note that for  $(u, v) \in \mathbb{R}_{>0}^2$  the matrix  $B(u, v)$  has one zero eigenvalue and one positive eigenvalue.

**Lemma 1.** *The eigenvalues of  $B(u, v)$  are*

$$\lambda_1 = 0, \quad \lambda_2 = \frac{\gamma uv}{(u+v)^2}$$

Regularizing (2.5) by including the additional diffusion terms  $\epsilon\Delta u$  and  $\epsilon\Delta v$  results in a *normally parabolic* diffusion system.

**Theorem 2.** *For all  $\epsilon > 0$ , the following PDE system is normally parabolic for strictly positive  $u, v$ .*

$$\begin{cases} \partial_t u = -\nabla \cdot (u\nabla f) + \epsilon\Delta u, & \text{in } \Omega \times (0, T) \\ \partial_t v = -(1 + \gamma)\nabla \cdot (v\nabla f) + \epsilon\Delta v, & \text{in } \Omega \times (0, T), \\ \nu \cdot (u\nabla f - \epsilon\nabla u) = \nu \cdot (v\nabla f - \epsilon\nabla v) = 0, & \text{on } \partial\Omega \times (0, T), \\ u(x, 0) = u_0(x) > 0, & \text{in } \Omega, \\ v(x, 0) = v_0(x) > 0, & \text{in } \Omega, \end{cases} \quad (2.8)$$

*Proof.* Note that for the regularized PDE system in (2.8), the matrix of coefficients  $B_\epsilon(u, v)$  is

$$B_\epsilon = B(u, v) + \epsilon I$$

having the eigenvalues  $\lambda_1 = \epsilon$  and  $\lambda_2 = \frac{\gamma uv}{(u+v)^2} + \epsilon$ . These eigenvalues are strictly positive for  $u, v \in \mathbb{R}_{>0}^2$ .

The set

$$G = \{\xi \in \mathbb{R}^2 : \sigma(B_\epsilon(\xi)) \subset [\operatorname{Re} z > 0]\}$$

clearly contains  $\mathbb{R}_{>0}^2$ . Since the PDE system also satisfies (1.6)-(1.7) in this region, it follows that (2.8) is normally parabolic for strictly positive  $u, v$ .  $\square$

**Corollary 1.** *Given strictly positive initial conditions  $u_0$  and  $v_0$  and taking  $\mathbf{u}(t) = (u(t), v(t)) \in C(\bar{\Omega})$ , (2.8) has a unique maximal solution*

$$\mathbf{u}(\cdot) \in C([0, t_f]) \cap C^\infty(\bar{\Omega} \times (0, t_f), \mathbb{R}^d). \quad (2.9)$$

*Proof.* This follows directly from Theorem 1. □

*Remark.* Note that  $B(u, v)$  in (2.7) is not symmetric and our resulting PDE is non-coercive. Nonetheless, under our assumptions, the perturbed system involving  $B_\epsilon(u, v)$  satisfies the conditions to be normally parabolic having smooth, local in time solutions.

### 3 A simple system: two coupled spatial points

It is instructive to consider a discrete spatial model for the fitness-gradient flux, where population movements can be described by a system of ordinary differential equations (ODE). Here we consider two populations moving between two nodes. In analogy to the system described by (2.5), movement of each population is determined by a fitness gradient; simply put, movement is toward the node where population fitness is higher. As in Section 2, fitness is defined by the expected payoff of an underlying evolutionary game between the two populations, and we again imagine the dynamic as movement of a prey population, with density given by  $u$  and a predator population, whose density is given by  $v$ .

In this context, fitness depends only on the population ratio  $u/v$  at each node. A steady state is reached when these ratios are equal between nodes, or when both populations accumulate at a single node, leaving the other node empty. In other words, the prey either distributes its population between nodes so that it is in constant ratio to the predator population, or the entire prey population aggregates to a single node, followed by

As we show, the system approaches a steady state for any initial conditions and for particular initial conditions, both populations accumulate on a single node. This is perhaps the most interesting behavior of this basic model as it provides some insight into the pinching off behavior observed the fitness-gradient flux PDE system for two populations given by (2.5).

For  $i = 1, 2$ , let  $u_i(t)$  and  $v_i(t)$  denote populations at node  $i$  at time  $t \geq 0$ . In the model under consideration, population changes are due entirely

to migration between nodes, as described by the following system of ODEs:

$$\dot{u}_1 = \begin{cases} u_2 [f_1(u_1, v_1) - f_1(u_2, v_2)], & \text{if } f_1(u_1, v_1) \geq f_1(u_2, v_2), \\ -u_1 [f_1(u_2, v_2) - f_1(u_1, v_1)], & \text{if } f_1(u_1, v_1) < f_1(u_2, v_2), \end{cases} \quad (3.1)$$

$$\dot{v}_1 = \begin{cases} \beta v_2 [f_2(u_1, v_1) - f_2(u_2, v_2)], & \text{if } f_2(u_1, v_1) \geq f_2(u_2, v_2), \\ -\beta v_1 [f_2(u_2, v_2) - f_2(u_1, v_1)], & \text{if } f_2(u_1, v_1) < f_2(u_2, v_2), \end{cases} \quad (3.2)$$

$$\dot{u}_2 = -\dot{u}_1, \quad (3.3)$$

$$\dot{v}_2 = -\dot{v}_1. \quad (3.4)$$

The function  $f_1(u, v)$  describes a fitness for  $u$  that depends only on the relative size of the populations  $u$  and  $v$  (at a given node). Similarly,  $f_2(u, v)$  describes the fitness of  $v$ . The parameter  $\beta > 0$  indicates the degree to which population  $v$  is sensitive to a difference in fitness, relative to population  $u$ 's sensitivity, as discussed in Section 2.

For each population, migration between the nodes corresponds to movement in the direction of increasing fitness. Fixed points of the system occur when the fitness of both species is equal between the two nodes. For our definition of fitness, this occurs when the populations satisfy

$$u_1 v_2 = u_2 v_1.$$

This occurs when the population ratios at each node are equal or when both populations accumulate at a single node, as discussed below.

As in 2, we take

$$f_1(u, v) = \frac{a_{11}u + a_{12}v}{u + v}, \quad f_2(u, v) = \frac{a_{21}u + a_{22}v}{u + v}, \quad (3.5)$$

and set

$$a_{11} - a_{12} = 1, \quad \kappa_A = a_{21} - a_{22} > 0 \quad (3.6)$$

Let  $\delta f$  denote the difference in fitness for population  $u$  between the two nodes,

$$\delta f = f_1(u_1, v_1) - f_1(u_2, v_2).$$

Then using (3.5), (3.6) we have

$$\begin{aligned} \delta f &= \frac{1}{(u_1 + v_1)(u_2 + v_2)} (u_1 v_2 - u_2 v_1), \\ \kappa_A \delta f &= f_2(u_1, v_1) - f_2(u_2, v_2), \end{aligned} \quad (3.7)$$

Again as in Section 2, we make the assumption  $\beta\kappa_A > 1$ , and define the positive parameter  $\gamma$  by

$$\gamma = \beta\kappa_A - 1 > 0. \quad (3.8)$$

This allows us to re-write (3.1)-(3.2) in terms of  $\delta f$ ; effectively, population  $v$  is more sensitive than  $u$  to differences in  $f$  between the two nodes.

$$\dot{u}_1 = \begin{cases} u_2\delta f, & \text{if } \delta f \geq 0, \\ u_1\delta f, & \text{if } \delta f < 0, \end{cases} \quad (3.9)$$

$$\dot{v}_1 = \begin{cases} (1 + \gamma)v_2\delta f, & \text{if } \delta f \geq 0, \\ (1 + \gamma)v_1\delta f, & \text{if } \delta f < 0, \end{cases} \quad (3.10)$$

$$\dot{u}_2 = -\dot{u}_1, \quad (3.11)$$

$$\dot{v}_2 = -\dot{v}_1, \quad (3.12)$$

$$u_i(0) = u_i^0 > 0, \quad v_i(0) = v_i^0 > 0, \quad \text{for } i = 1, 2. \quad (3.13)$$

*Remark.* In our reduced model, the assumption  $\gamma > 0$  implies that the population  $v$  is more sensitive to (or responds more rapidly to a change in) the difference in fitness,  $\delta f$ . This assumption is important for the parabolic nature of the PDE discussed in Section 2.

*Remark.* From (3.7), we see that  $u_1v_2 = u_2v_1$  implies  $\delta f = 0$  and hence  $\dot{u}_i = \dot{v}_i = 0$ . Motivated by this condition, we define  $E(t) := u_1v_2 - u_2v_1$ , so that the ODE system (3.9)-(3.13) is at a steady state when  $E = 0$ . We show that  $E \xrightarrow{t \rightarrow \infty} 0$ , for any positive initial conditions. Furthermore, for some initial conditions, the total population accumulates at one node with the other node emptying out.

Let us denote the total population at each node  $i$  at time  $t$  by  $S_i(t)$ ,

$$S_1(t) = u_1(t) + v_1(t),$$

$$S_2(t) = u_2(t) + v_2(t).$$

Because the populations  $u_1 + u_2$  and  $v_1 + v_2$  are conserved, there is a bound on each  $u_i$  and  $v_i$  and hence on the product  $S_1S_2$ . Therefore there exists a constant  $M > 0$  such that for all  $t \geq 0$ ,

$$S_1(t)S_2(t) \leq M.$$

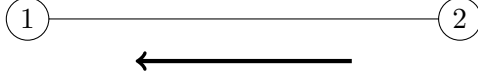


Figure 1: Schematic of the two node model. The arrow denotes the direction of flux for  $u$  when  $E > 0$  (equivalently when  $\delta f > 0$ ).

**Lemma 2.** *For any initial conditions  $u_i(0), v_i(0) > 0$  for  $i = 1, 2$ , the ODE system (3.9)-(3.13) converges to a steady state such that  $E = u_1 v_2 - u_2 v_1 = 0$ .*

*Proof.* Again we assume that  $\delta f$  is positive at  $t = 0$ . Then

$$\begin{cases} \dot{u}_1 = u_2 \delta f, \\ \dot{v}_1 = (1 + \gamma) v_2 \delta f, \\ \dot{u}_2 = -\dot{u}_1, \\ \dot{v}_2 = -\dot{v}_1, \end{cases}$$

and  $E(0) = (u_1 v_2 - u_2 v_1) > 0$ , since  $\delta f > 0$ . Next,

$$\begin{aligned} \dot{E} &= \dot{u}_1 v_2 + u_1 \dot{v}_2 - \dot{u}_2 v_1 - u_2 \dot{v}_1 \\ &= \dot{u}_1 (v_1 + v_2) - \dot{v}_1 (u_1 + u_2) \\ &= u_2 (v_1 + v_2) \delta f - (1 + \gamma) v_2 (u_1 + u_2) \delta f \\ &= [(u_2 v_1 - u_1 v_2) - \gamma v_2 (u_1 + u_2)] \delta f \\ &\leq -E \delta f \\ &= -\frac{1}{S(t)T(t)} E^2 \leq -\frac{1}{M} E^2. \end{aligned}$$

Thus,

$$\dot{E} \leq -CE^2$$

for some  $C > 0$ , which implies that  $E(t) \xrightarrow{t \rightarrow \infty} 0$ . To see this define

$$F(t) = \frac{E(0)}{Ct + 1},$$

and note that  $F(0) = E(0)$ ,  $\dot{E} \leq \dot{F}$ , and  $F(t) \xrightarrow{t \rightarrow \infty} 0$ .  $\square$

Since  $u_1$  and  $v_1$  are initially increasing (for  $E(0) > 0$ ), we have in the limit

$$\frac{u_1}{v_1} v_2 = u_2.$$

If  $v_2 > E$  at  $t = 0$ , then  $v_2$  and  $u_2$  remain bounded away from zero and the steady state condition can also be written

$$\frac{u_1}{v_1} = \frac{u_2}{v_2}.$$

When  $v_2 \leq E$  at  $t = 0$ , however, we will show that node 2 empties out, as the entire population moves to node 1. Consider the projection of trajectories to the  $(v_2, E)$ -phase plane (see Figure 2), for which

$$\frac{dE}{dv_2} = \frac{\dot{E}}{\dot{v}_2} = \frac{E + \gamma v_2}{(1 + \gamma)v_2} = \frac{1}{(1 + \gamma)v_2} E + \frac{\gamma}{(1 + \gamma)}. \quad (3.14)$$

Notice that when  $E(t) = v_2(t)$ , then

$$\frac{dE}{dv_2} = 1,$$

so that the trajectory remains along the line  $v_2 = E$ , approaching the origin as  $t \rightarrow \infty$ . This line divides the phase plane into two regions that characterize the asymptotic behavior. Trajectories for which  $E \geq v_2$  at  $t = 0$  (i.e. begin on or above the line  $E = v_2$ ) will also approach the origin, while trajectories with  $E < v_2$  at  $t = 0$  (beginning below the line) approach a positive value of  $v_2$  along the  $v_2$ -axis - see Figure 2.

If we make a normalization so that  $u_1 + u_2 = 1$ , then we can write the explicit solution to (3.14) for  $E$  as a function of  $v_2$  is

$$E(v_2) = v_2 + (\alpha - 1)v_2^{\frac{1}{1+\gamma}}, \quad (3.15)$$

where  $\alpha$  is a parameter that characterizes the trajectories. We use  $v_2 = 1$  as a reference value in the  $(v_2, E)$ -plane, and let  $\alpha$  denote  $E(1)$ , the value of  $E$  when  $v_2 = 1$ , which will depend on the initial conditions. Specifically, if  $E_0$  and  $v_2^0$  denote the values of  $E$  and  $v_2$  at time  $t = 0$ , then

$$\alpha = \frac{E_0 - v_2^0}{(v_2^0)^{\frac{1}{1+\gamma}}} + 1.$$

Recall from (3.9)-(3.13) that  $v_2$  and  $E$  are decreasing whenever  $E > 0$ . The choice  $\alpha = 1$  corresponds to the trajectory along the line  $E = v_2$ . When  $\alpha > 1$ , the trajectory lies above the line  $E = v_2$  and approaches the origin as  $t \rightarrow \infty$ . When  $\alpha < 1$ , the trajectory is below the line  $E = v_2$ , intersecting the  $v_2$ -axis at  $v_2 = (1 - \alpha)^{\frac{1+\gamma}{\gamma}}$ . We summarize these results in the theorem below.

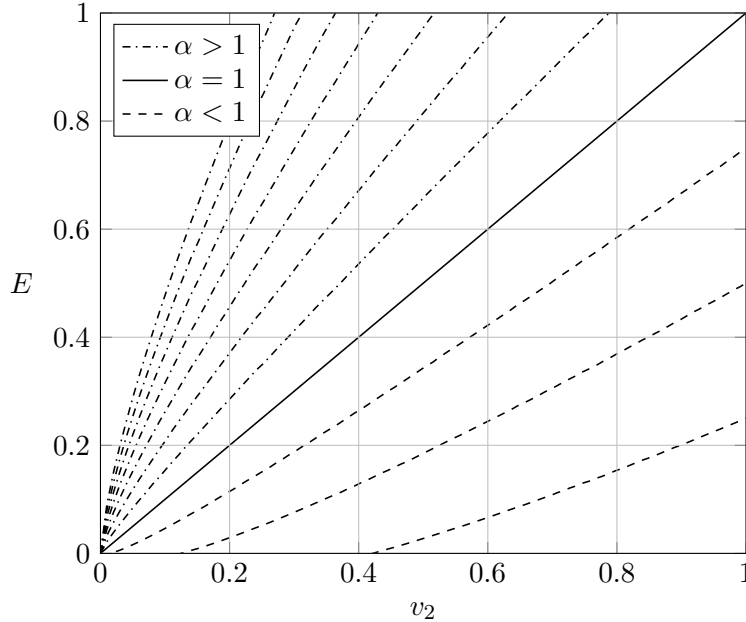


Figure 2: ODE dynamics in the  $(v_2, E)$ -plane, for  $\gamma = 0.5$  and  $E > 0$  at  $t = 0$ . Trajectories satisfy (3.15), with  $\alpha$  determined by the initial conditions ( $\alpha = E(1)$ ). For  $\alpha > 1$ , trajectories approach the origin as  $t \rightarrow \infty$ . For  $\alpha = 1$ , the trajectory approaches the origin along the line  $E = v_2$ . Trajectories for  $\alpha < 1$  approach the point  $\left( (1 - \alpha)^{\frac{1+\gamma}{\gamma}}, 0 \right)$  along the  $v_2$ -axis.

**Theorem 3.** Define  $E(t) = u_1 v_2 - u_2 v_1$ . If  $-v_1(0) < E(0) < v_2(0)$ , then the ODE system (3.9)-(3.13) approaches a steady state such that

$$\frac{u_1}{v_1} = \frac{u_2}{v_2}. \quad (3.16)$$

If  $v_2(0) \leq E(0)$ , then  $u_2, v_2 \rightarrow 0$ , whereas if  $v_1(0) \leq -E(0)$ , then  $u_1, v_1 \rightarrow 0$ .

## 4 Derivation of the fitness gradient flux PDE

In this section we derive the fitness gradient flux PDE (1.1) in two dimensions; this system was first described in [15]. Our derivation is similar to continuum limit arguments for biased random walks that appear in [29, 35].

Biased random walks in theoretical populations are discussed in greater detail in [37].

Let  $\{x_{ij}\}$  denote a  $J_x \times J_y$  uniform grid with uniform meshsize  $\delta x$ . At time  $t$ , each grid point  $x_{ij}$  has populations  $u(x_{ij}, t)$  and  $v(x_{ij}, t)$ . Our model is based on the following assumption: the movement of each population on this grid is governed by transition probabilities, which are proportional to local differences in fitness, and defined in the following.

**Definition 1.** Given two grid points  $a$  and  $b$ , and fixed timestep  $\delta t$ , we define the transition probability  $p(a, b; t)$  to be the probability that an individual from population  $u$  moves from  $a$  to  $b$  in the time interval  $(t, t + \delta t)$ . We define an analogous transition probability  $q(a, b; t)$  for the population  $v$ .

Note that the allowed transitions will be made effectively local by restricting points  $a$  and  $b$  to be nearest neighbors on the grid. We use the following notation conventions throughout this section.

**Notation.** For lattice nodes denoted by  $a$ ,  $x_{ij}$ , or  $x_\alpha$  with  $\alpha \in \{(i, j - 1), (i, j + 1), (i - 1, j), (i + 1, j)\}$ , let

$$u_a^t := u(a, t), \quad u_{ij}^t = u(x_{ij}, t), \quad u_\alpha^t = u(x_\alpha, t),$$

and similarly for the fitness functions  $f(u, v)$ ,  $g(u, v)$ , let

$$f_{ij}^t = f(u_{ij}^t, v_{ij}^t).$$

We also define the following forward-difference and backward difference operators

$$\begin{aligned} D_x^+ u_{ij} &= \frac{1}{\delta x} (u_{i+1,j} - u_{ij}), \\ D_y^+ u_{ij} &= \frac{1}{\delta x} (u_{i,j+1} - u_{ij}), \\ D_x^- u_{ij} &= \frac{1}{\delta x} (u_{ij} - u_{i-1,j}), \\ D_y^- u_{ij} &= \frac{1}{\delta x} (u_{ij} - u_{i,j-1}). \end{aligned}$$

**Definition 2.** Let  $a$  and  $b$  be adjacent nodes and let the fitness functions  $f$  and  $g$  be bounded continuous functions. Define the bounds

$$M_1 = \{\sup \mathbf{f}(\mathbf{x}) - \inf \mathbf{f}(\mathbf{x})\}, \quad M_2 = \{\sup \mathbf{g}(\mathbf{x}) - \inf \mathbf{g}(\mathbf{x})\},$$

where the sup and inf are taken over  $\mathbf{x} \in \mathbb{R}^+ \times \mathbb{R}^+$  (the domain of the fitness functions). We define the transition probabilities  $p(a, b; t)$  and  $q(a, b; t)$  to depend on the fitness differences as

$$\begin{aligned} p(a, b; t) &= \begin{cases} \frac{1}{4M_1}(f_b^t - f_a^t), & \text{if } f_b^t \geq f_a^t, \\ 0, & \text{if } f_b^t < f_a^t, \end{cases} \\ q(a, b; t) &= \begin{cases} \frac{1}{4M_2}(g_b^t - g_a^t), & \text{if } g_b^t \geq g_a^t, \\ 0, & \text{if } g_b^t < g_a^t. \end{cases} \end{aligned} \quad (4.1)$$

Note that in this formulation, at most one of  $p(a, b; t)$  or  $p(b, a; t)$  can be nonzero, representing the fact that an individual has nonzero probability of moving to an adjacent node if and only if the fitness is strictly higher at that node. Thus, populations travel to adjacent points by moving in the direction of increasing fitness, as in the two-node model of Section 3.

The scaling constants,  $\frac{1}{4M_1}$  and  $\frac{1}{4M_2}$ , ensure that for any node  $x_{ij}$ ,

$$\sum_{\alpha} p(x_{ij}, x_{\alpha}; t) \leq 1, \quad \text{and} \quad \sum_{\alpha} q(x_{ij}, x_{\alpha}; t) \leq 1,$$

where  $\alpha$  ranges over the set of nodes adjacent to  $x_{ij}$ .

We now derive the PDE for the population density  $u$ ; the argument for  $v$  is entirely similar. Consider  $u$  at the node  $x_{ij}$  and at time  $t + \delta t$ :

$$\begin{aligned} u(x_{ij}, t + \delta t) &= u_{ij}^t + \frac{1}{4M_1} \sum_{\alpha} u_{\alpha}^t p(x_{\alpha}, x_{ij}; t) - \frac{1}{4M_1} \sum_{\alpha} u_{ij}^t p(x_{ij}, x_{\alpha}; t) \\ &= u_{ij}^{t+\delta t}. \end{aligned}$$

With respect to either coordinate direction, the fitness function  $f$  may be increasing, decreasing, or achieve a local extremum at  $x_{ij}$ . We show the case where the fitness function  $f$  is increasing with respect to both coordinate directions.

$$f_{i+1,j}^t \geq f_{ij}^t \geq f_{i-1,j}^t, \quad f_{i,j+1}^t \geq f_{ij}^t \geq f_{i,j-1}^t.$$

$$\begin{aligned}
u_{ij}^{t+\delta t} - u_{ij}^t &= \frac{1}{4M_1} u_{i-1,j}^t (f_{ij}^t - f_{i-1,j}^t) - \frac{1}{4M_1} u_{ij}^t (f_{i+1,j}^t - f_{ij}^t) \\
&\quad + \frac{1}{4M_1} u_{i,j-1}^t (f_{ij}^t - f_{i,j-1}^t) - \frac{1}{4M_1} u_{ij}^t (f_{i,j+1}^t - f_{ij}^t), \\
\frac{u_{ij}^{t+\delta t} - u_{ij}^t}{\delta t} &= \left( \frac{\delta x^2}{4M_1 \delta t} \right) \left( \frac{u_{i-1,j}^t}{\delta x} \left( \frac{f_{ij}^t - f_{i-1,j}^t}{\delta x} \right) - \frac{u_{ij}^t}{\delta x} \left( \frac{f_{i+1,j}^t - f_{ij}^t}{\delta x} \right) \right) \\
&\quad + \left( \frac{\delta x^2}{4M_1 \delta t} \right) \left( \frac{u_{i,j-1}^t}{\delta x} \left( \frac{f_{ij}^t - f_{i,j-1}^t}{\delta x} \right) - \frac{u_{ij}^t}{\delta x} \left( \frac{f_{i,j+1}^t - f_{ij}^t}{\delta x} \right) \right) \\
&= \frac{\delta x^2}{4M_1 \delta t} \left( \frac{u_{i-1,j}^t}{\delta x} D_x^+ f_{i-1,j}^t - \frac{u_{ij}^t}{\delta x} D_x^+ f_{ij}^t \right) \\
&\quad + \frac{\delta x^2}{4M_1 \delta t} \left( \frac{u_{i,j-1}^t}{\delta x} D_y^+ f_{i,j-1}^t - \frac{u_{ij}^t}{\delta x} D_y^+ f_{ij}^t \right) \\
&= \frac{\delta x^2}{4M_1 \delta t} \left[ -D_x^- (u_{ij}^t D_x^+ f_{ij}^t) - D_y^- (u_{ij}^t D_y^+ f_{ij}^t) \right].
\end{aligned}$$

Since, by assumption,  $-D_x^+ f_{ij} < 0$  and  $-D_y^+ f_{ij} < 0$ , we notice that the backward-difference operator in the final line is equivalent to a first-order upwinding scheme [25]. Consideration of the other cases bears this out. Therefore, by taking a limit as  $\delta t \rightarrow 0$  and  $\delta x \rightarrow 0$  in such a way that

$$\lim_{\substack{\delta t \rightarrow 0 \\ \delta x \rightarrow 0}} \frac{\delta x^2}{\delta t} = 1,$$

we arrive at the fitness gradient equation in (1.1), and given below in (5.1), where  $\beta_1 = \frac{1}{4M_1}$  and  $\beta_2 = \frac{1}{4M_2}$ .

## 5 Analysis of the Fitness Gradient Flux System

In this section we analyze the system

$$\begin{cases}
\partial_t u = -\nabla \cdot (u \nabla f), & \text{in } \Omega \times (0, T), \\
\partial_t v = -(1 + \gamma) \nabla \cdot (v \nabla f) & \text{in } \Omega \times (0, T), \\
\nu \cdot (u \nabla f) = 0, \quad \nu \cdot (v \nabla f) = 0, & \text{on } \partial\Omega \times (0, T), \\
u(\mathbf{x}, 0) = u_0(\mathbf{x}) > 0, & \text{in } \Omega, \\
v(\mathbf{x}, 0) = v_0(\mathbf{x}) > 0, & \text{in } \Omega.
\end{cases} \quad (5.1)$$

*Remark.* Under our assumptions, the populations  $u$  and  $v$  experience the same fitness gradient  $\nabla f$ , but the population  $v$  has a higher sensitivity to the gradient than does  $u$ , since  $\gamma > 0$ . The game dynamics lead the population  $u$  to aggregate, and to flee regions where the density of  $v$  is high, while the population  $v$  pursues  $u$ . Due to the  $v$  population's higher sensitivity, it is it acts to inhibit  $u$ 's aggregation. If  $\gamma < 0$  however, then (5.1) is ill-posed.

As discussed in Section 2, we may write (5.1) as

$$\partial_t \mathbf{w} = \nabla \cdot (B(\mathbf{w}) \nabla \mathbf{w}), \quad (5.2)$$

where  $\mathbf{w} = (u, v)$  and  $\nabla \mathbf{w} = (\nabla u, \nabla v)$  and

$$B(u, v) = (b_{ij}(u, v)) = \frac{1}{(u+v)^2} \begin{bmatrix} -uv & u^2 \\ -(1+\gamma)v^2 & (1+\gamma)uv \end{bmatrix}. \quad (5.3)$$

## 5.1 Steady State Solutions

As was previously observed in [15], strictly positive steady state solutions are characterized by the simple condition  $u = cv$ . When  $u$  and  $v$  are smooth positive functions on  $\overline{\Omega}$ , then we have the following:

**Theorem 4.** *Let  $u$  and  $v$  be strictly positive functions in  $C^1(\overline{\Omega})$ . Then  $(u, v)$  is a steady state solution of (5.1) if and only if  $u = cv$ , where*

$$c = \frac{\|u\|_{L^1(\Omega)}}{\|v\|_{L^1(\Omega)}}.$$

*Proof.* Given  $u = cv$ , then using  $\ln u = \ln(cv)$  one has

$$\frac{\nabla u}{u} = \frac{\nabla v}{v},$$

or

$$v \nabla u - u \nabla v = 0.$$

From (2.4) this implies  $\nabla f = \mathbf{0}$  and thus  $\partial_t u = \partial_t v = 0$ . Note that this also implies that the fitness function  $f$  is constant.

Conversely, if  $(u, v)$  is a steady state solution, then

$$\begin{aligned} \nabla \cdot (u \nabla f) &= 0, \\ (1 + \gamma) \nabla \cdot (v \nabla f) &= 0. \end{aligned}$$

This implies

$$\begin{aligned} -\nabla u \cdot \nabla f &= u \Delta f, \\ -\nabla v \cdot \nabla f &= v \Delta f. \end{aligned}$$

Consequently,

$$-\frac{\nabla u}{u} \cdot \nabla f = \Delta f = -\frac{\nabla v}{v} \cdot \nabla f, \quad (5.4)$$

and

$$(v \nabla u - u \nabla v) \cdot \nabla f = 0. \quad (5.5)$$

Recalling the value of  $\nabla f$  from (2.4), we have

$$\frac{1}{(u+v)^2} |v \nabla u - u \nabla v|^2 = 0.$$

Since by our assumptions  $\frac{1}{(u+v)^2} > 0$ , we conclude

$$v \nabla u - u \nabla v = 0.$$

Equivalently,

$$\nabla \ln u = \nabla \ln v,$$

which implies  $\ln u = \ln(cv)$  and  $u = cv$ . Since

$$\int_{\Omega} u dx = \int_{\Omega} cv dx,$$

with  $u, v > 0$ , it is easy to see that  $c$  will be the ratio of the  $L^1$  norms. □

## 5.2 Weak Steady State Solutions

If  $\Omega$  is an interval, we can define continuous weak steady state solutions in  $H^1(\Omega)$ . As shown above, when  $u = cv$ , then we have  $\partial_x f = 0$ ; equivalently  $f$  constant. This is a local condition; it possible that  $f$  is only piece-wise constant. If  $u$  and  $v$  are to be continuous, we must have  $u = v = 0$  at points of discontinuity of  $f$ .

For example, suppose that  $\Omega$  is partitioned into two disjoint intervals:  $\Omega = (x_0, x_1] \cup (x_1, x_2) = I_1 \cup I_2$  and let  $u = c_1 v$  on  $I_1$  and  $u = c_2 v$  on  $I_2$ . If each  $u$  and  $v$  are to be continuous we must have  $u = v = 0$  at the adjoining endpoint  $x_1$ . In this case, we have  $\partial_x f = 0$  everywhere except at  $x_1$  (where  $\partial_x f$  is not defined). The resulting  $(u, v)$  is a weak steady state solution of (5.1).

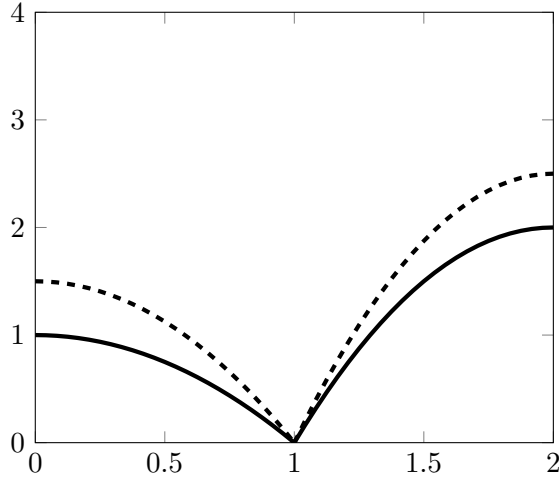


Figure 3:  $u$  and  $v$ ,  $v = 1.5u$  on  $(0, 1)$  and  $v = 1.25u$  on  $(1, 2)$

If we partition  $\Omega$  into a set of disjoint intervals, then  $f$  may have a different constant value on each interval, with  $u = v = 0$  at the adjoining endpoints. An example is shown in Figures 5.2 and 5.2.

**Definition 3.** For functions  $u$  and  $v$  in  $H^1(\Omega)$ ,  $(u, v)$  is a weak steady state solution of (5.1) if, for every pair of smooth test functions  $\phi, \psi \in C_0^\infty(\Omega)$ ,

$$\begin{aligned} \int_{\Omega} \phi_x \cdot (u f_x) dx &= 0, \\ \int_{\Omega} \psi_x \cdot (v f_x) dx &= 0. \end{aligned} \tag{5.6}$$

**Theorem 5.** Let  $\Omega$  be a bounded open interval in  $\mathbb{R}$ . Let  $v \in H^1(\Omega)$ , with  $v \geq 0$  and such that  $v = 0$  at no more than a finite number of points  $x_k \in \Omega$ . This set of zeros partitions  $\Omega$  into a finite collection of disjoint intervals  $I_k$ .

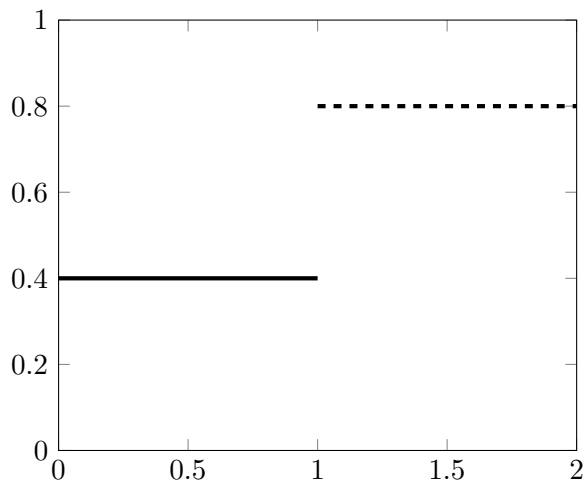


Figure 4: Piecewise-constant  $f$

Construct a function  $u$  as follows. For each interval  $I_k$ , let  $c_k$  be a nonnegative constant and take  $u=c_kv$  on  $I_k$ . Then  $(u, v)$  is a weak steady state solution of (5.1).

*Proof.* By construction for each  $k$ , we have  $\nabla f = 0$  on each interval  $I_k$ . Since  $u$  and  $v$  are each in  $H^1(\Omega)$ , we can take  $u$  and  $v$  to be absolutely continuous. Therefore  $u(x_k) = v(x_k) = 0$ .

Take  $\phi \in C_0^\infty(\Omega)$  and consider

$$\int_{\Omega} \phi \nabla \cdot (u \nabla f) dx = - \int_{\Omega} \nabla \phi \cdot (u \nabla f) dx$$

Although  $u \in H^1(\Omega)$ , the function  $f$  under our assumptions is piecewise constant and consequently is not in  $H^1(\Omega)$ . Suppose that  $f$  has one point of discontinuity at  $x_1 \in \Omega = (x_0, x_2)$ , as in 5.2 and consider a small open interval around this point  $B(x_1, \epsilon)$ . Then

$$\begin{aligned} - \int_{\Omega} \nabla \phi \cdot (u \nabla f) dx &= - \int_{x_0}^{x_1-\epsilon} \nabla \phi \cdot (u \nabla f) dx - \int_{x_1+\epsilon}^{x_2} \nabla \phi \cdot (u \nabla f) dx \\ &\quad - \int_{x_1-\epsilon}^{x_1+\epsilon} \nabla \phi \cdot (u \nabla f) dx. \end{aligned}$$

By assumption,  $\nabla f = 0$  on  $(x_0, x_1 - \epsilon)$  and  $(x_1 + \epsilon, x_2)$ . Thus we have

$$\begin{aligned}
-\int_{x_1-\epsilon}^{x_1+\epsilon} \nabla \phi \cdot (u \nabla f) dx &= -\int \nabla f \cdot (u \nabla \phi) dx \\
&= \int_{x_1-\epsilon}^{x_1+\epsilon} \nabla \cdot (u \nabla \phi) f dx - (u \nabla \phi f)(x_1 + \epsilon) + (u \nabla \phi f)(x_1 - \epsilon) \\
&= \int_{x_1-\epsilon}^{x_1+\epsilon} u \Delta \phi f + \nabla u \cdot \nabla \phi f dx - (u \nabla \phi f)(x_1 + \epsilon) + (u \nabla \phi f)(x_1 - \epsilon)
\end{aligned}$$

Note that  $f(u)$  is not defined when  $u = v = 0$ , but  $f$  is bounded as  $(u, v) \rightarrow (0, 0)$ . Since  $u$  and  $v$  are in  $\in H_1(\Omega)$ , we have, for some constant  $C$ ,

$$\left| \int_{\Omega} \nabla \phi (u \nabla f) dx \right| \leq \epsilon C \|u\|_{H^1(\Omega)} \|\phi\|_{H^1(\Omega)} \rightarrow 0 \text{ as } \epsilon \rightarrow 0.$$

Similarly, we have  $\int_{\Omega} \phi \nabla \cdot (v \nabla f) dx = 0$  so that  $(u, v)$  is a weak solution of (5.1).  $\square$

*Remark.* Although the piecewise constant function  $f$  does not have a weak derivative, its distributional derivative is a delta function (or a finite set of delta functions in the general case). Integrating the function  $u$  against  $\nabla f$  thus gives us the value  $u(x_1)$ , which by our assumptions is zero. Thus we see (again) that it is essential that the function  $u = 0$  at each point  $x_k$  where the fitness  $f$  is discontinuous.

*Remark.* For the model in (2.5) below, describing two populations, numerical simulations have shown that for some initial conditions, the system evolves to such weak steady state solutions. A 'pinching off' occurs, where each population reaches zero at a point in  $\Omega$ . The populations then redistribute themselves on the remaining subintervals, until reaching a configuration where  $\nabla f = 0$  on each subinterval.

*Remark.* The consideration of weak steady state solutions reveals two shortcomings in our model. First, there is no law of motion for the population  $u$  in the absence of  $v$ , or vice versa (since the fitness is constant in that case). If  $u_0 = 0$  on some subinterval  $I \subset \Omega$ , then  $(u_0, v_0)$  will be a weak steady state solution to (5.1), provided  $u_0$  and  $v_0$  are in  $H^1(\Omega)$ , satisfy the Neumann boundary condition, and

$$u_0 = cv_0 \text{ in } \Omega \setminus I. \tag{5.7}$$

That is,  $v_0$  can be arbitrarily chosen on the subinterval  $I$  where  $u_0 \equiv 0$ .

Second, our fitness derives from an evolutionary game, which is inherently a mean-field model. The evolutionary game approach assumes large well-mixed populations, but these assumptions break down when  $u + v \ll 1$ . An improved model would require multiple scales, where the mean-field approach dominates when  $u$  and  $v$  are large, while dynamics for individual interactions are brought into play when  $u$  and  $v$  are near zero.

In future work we may consider alterations to these models that address these shortcomings.

### 5.3 Linearization around a steady state

We next study solutions for a linearization of the fitness-flux PDE in the case of two populations, and where  $\Omega$  is an interval. Solutions are of the form

$$\mathbf{w}(x, t) = (u(x, t) - u_0(x), v(x, t) - v_0(x)),$$

where  $(u_0, v_0)$  is a smooth (strictly positive), steady state solution to (2.5). We show that this steady state is neutrally. While perturbations from the steady state remain bounded, they do not decay but tend toward a new steady state near  $(u_0, v_0)$  in the  $L^2$  sense.

We choose  $\Omega$  to be the interval  $(0, 2\pi)$ ;  $u_0$  and  $v_0$  are strictly positive, and  $u_0 = cv_0$  with  $c = \|u_0\| / \|v_0\|$  as before. We consider the linearization

$$\begin{aligned}\partial_t w_1 &= \nabla \cdot [\partial_u P(u_0, v_0)w_1 + \partial_v P(u_0, v_0)w_2] \\ \partial_t w_2 &= \nabla \cdot [\partial_u Q(u_0, v_0)w_1 + \partial_v Q(u_0, v_0)w_2],\end{aligned}$$

Where

$$\begin{aligned}P(u, v) &= \nabla \cdot [b_{11}(u, v)\nabla u + b_{12}(u, v)\nabla v] \\ Q(u, v) &= \nabla \cdot [b_{21}(u, v)\nabla v + b_{22}(u, v)\nabla v],\end{aligned}$$

$$\begin{aligned}\partial_u P(u, v)w_1 &= \nabla \cdot \left[ \frac{uv - v^2}{(u + v)^3} w_1 \nabla u - \frac{uv}{(u + v)^2} \nabla w_1 + \frac{2uv}{(u + v)^3} w_1 \nabla v \right] \\ \partial_v P(u, v)w_2 &= \nabla \cdot \left[ \frac{uv - u^2}{(u + v)^3} w_2 \nabla u + \frac{u^2}{(u + v)^2} \nabla w_2 - \frac{2u^2}{(u + v)^3} w_2 \nabla v \right] \\ \partial_u Q(u, v)w_1 &= (1 + \gamma) \nabla \cdot \left[ \frac{2v^2}{(u + v)^3} w_1 \nabla u - \frac{v^2}{(u + v)^2} \nabla w_1 + \frac{v^2 - uv}{(u + v)^3} w_1 \nabla v \right] \\ \partial_v Q(u, v)w_2 &= (1 + \gamma) \nabla \cdot \left[ \frac{-2uv}{(u + v)^3} w_2 \nabla u + \frac{uv}{(u + v)^2} \nabla w_2 + \frac{u^2 - uv}{(u + v)^3} w_2 \nabla v \right]\end{aligned}$$

Evaluating the above at the steady state solution  $(cv_0, v_0)$ , we arrive at the following linearized PDE:

$$\begin{cases} \partial_t w_1 &= \frac{1}{(c+1)^2} \nabla \cdot \left[ (cw_1 - c^2 w_2) \frac{\nabla v_0}{v_0} - c \nabla w_1 + c^2 \nabla w_2 \right] \\ \partial_t w_2 &= \frac{(1+\gamma)}{(c+1)^2} \nabla \cdot \left[ (w_1 - cw_2) \frac{\nabla v_0}{v_0} - \nabla w_1 + c \nabla w_2 \right] \end{cases} \quad (5.8)$$

which can be written as

$$\partial_t \mathbf{w} = K \nabla \cdot \left( B \nabla \mathbf{w} - \frac{\nabla v_0}{v_0} B \mathbf{w} \right)$$

for

$$K = \frac{1}{(c+1)^2}, \quad \mathbf{w} = (w_1, w_2), \quad \text{and} \quad B = \begin{pmatrix} -c & c^2 \\ -(1+\gamma) & (1+\gamma)c \end{pmatrix}$$

The eigenvalues of  $B$  are  $\lambda_0 = 0$  and  $\lambda_1 = \gamma K c > 0$ , with corresponding eigenvectors

$$\mathbf{e}_0 = \begin{bmatrix} c \\ 1 \end{bmatrix}, \quad \mathbf{e}_1 = \begin{bmatrix} \frac{c}{1+\gamma} \\ 1 \end{bmatrix}.$$

Using the eigenvectors given above, we can decompose  $\mathbf{w}$  as

$$\mathbf{w}(x, t) = c_0(x, t) \mathbf{e}_0 + c_1(x, t) \mathbf{e}_1,$$

where  $c_0(x, t) \mathbf{e}_0$  is in the eigenspace associated with  $\lambda_0$  and, hence remains constant in time, while  $c_1(x, t)$  will evolve according to the linear PDE shown below (see equation (5.10)). Solving this system gives

$$\begin{aligned} c_0(x, t) &= \frac{1+\gamma}{c\gamma} w_1(x, t) - \frac{1}{\gamma} w_2(x, t), \\ c_1(x, t) &= -\frac{1+\gamma}{c\gamma} w_1(x, t) + \frac{1+\gamma}{\gamma} w_2(x, t). \end{aligned} \quad (5.9)$$

Given an initial condition  $\mathbf{w}_0(x, 0) = (w_1, w_2)$ , the function  $c_0(x, t) \mathbf{e}_0 = c_0(x, 0) \mathbf{e}_0$  is constant in time. Writing this as  $\mathbf{y}_0(x) = (y_0^1, y_0^2)$ , we have  $y_0^1 = c y_0^2$ , as we expect.

Writing  $\mathbf{y}_1(x, t) = c_1(x, t) \mathbf{e}_1$ , we see that  $\partial_t y_1^1 = \frac{c}{1+\gamma} \partial_t y_1^2$ . Thus, we can reduce the problem to the single linear partial differential equation,

$$\partial_t w = \alpha \Delta w - a(x) \nabla w - b(x) w, \quad \text{where} \quad \alpha = K \gamma c > 0, \quad (5.10)$$

and

$$a(x) = \alpha \frac{\nabla v_0}{v_0}, \quad b(x) = \alpha \left( \frac{\Delta v_0}{v_0} - \frac{|\nabla v_0|^2}{v_0^2} \right).$$

A perturbation attains a new steady state. We illustrate an example in Figure 8 in the next section.

We can also see the instability in the linearization by investigating a dispersion relation. We assume the solution takes the form  $w(x, t) = e^{i(\mathbf{k} \cdot \mathbf{x} + \omega t)}$ , with  $\omega \in \mathbb{C}$  and  $\mathbf{k}$  and  $\mathbf{x}$  in  $\mathbb{R}^n$ . Plugging this into (5.10) gives the dispersion relation

$$\frac{i\omega}{\alpha} = -|\mathbf{k}|^2 - i\mathbf{k} \cdot a(x) - b(x).$$

Thus, the real part of  $i\omega = -\alpha|\mathbf{k}|^2 - b(x)$ . Since  $b(x)$  is not positive in general, the modes for small wave-numbers, may grow on some parts of the domain  $\Omega$ , while for sufficiently large  $|k|$ , the associated modes will decay.

## 6 Discussion and Numerical Examples

To illustrate and provide insight into the results presented above, we next discuss several numerical examples in 1D. We discuss the numerical methods in Section 6.1. In Sections 6.2 - 6.3, we examine the transient and perturbation dynamics of steady states. In 6.4 we show several examples evolving to a weak steady state, with piecewise constant fitness. We conclude by demonstrating cross-diffusive instabilities and the onset of pattern formation produced when fitness gradient flux is included in a Lotka–Volterra type population model (Section 6.5).

### 6.1 Numerical Methods

We use an implicit numerical scheme by Newton iteration with a no-flux boundary condition; the discretization uses a first order upwinding scheme, necessary for simulating examples that evolve toward a weak steady state solution.

For the one-dimensional case, the PDE system (5.1) can be written as

$$\begin{aligned} u_t &= -u_x f_x - u f_{xx}, \\ v_t &= -(1 + \gamma)v_x f_x - (1 + \gamma)v f_{xx}. \end{aligned}$$

We describe the first-order upwinding discretization for  $u_t$ . The sign of  $f_x$  determines whether we use a forward or backward difference in the discretization of  $u_x$ : we use a backward difference when  $f_x > 0$  and a forward difference when  $f_x < 0$  [25].

Let  $f_{x,i}^+$  and  $f_{x,i}^-$  denote the forward and backward difference operators at  $x_i$ ,

$$f_{x,i}^+ = \frac{1}{\delta x} (f_{i+1} - f_i), \quad f_{x,i}^- = \frac{1}{\delta x} (f_i - f_{i-1}),$$

where  $f_i$  denotes  $f(x_i)$  (we are suppressing the time variable  $t$ ).

The first order central difference for  $f_{xx}$  can be computed as

$$f_{xx,i} = \frac{1}{\delta x} (f_{x,i}^+ - f_{x,i}^-).$$

If we use  $f_{x,i}^-$  whenever  $f_{x,i} > 0$  and  $f_{x,i}^+$  whenever  $f_{x,i} < 0$ , then we have the discretization

$$\partial_t u_i = \begin{cases} -u_{i+1} f_{x,i}^+ + u_i f_{x,i}^-, & f_{x,i} < 0, \\ -u_i f_{x,i}^+ + u_{i-1} f_{x,i}^-, & f_{x,i} > 0, \end{cases}$$

which we combine into

$$\partial_t u_i = -u_i f_{x,i}^+ [f_{x,i}^+ \geq 0] - u_{i+1} f_{x,i}^+ [f_{x,i}^+ < 0] + u_{i-1} f_{x,i}^- [f_{x,i}^- \geq 0] + u_i f_{x,i}^- [f_{x,i}^- < 0],$$

where

$$[g \geq 0] = \begin{cases} 1, & \text{if } g \geq 0, \\ 0, & \text{otherwise.} \end{cases}$$

*Remark.* If  $f_{x,i}^+$  and  $f_{x,i}^-$  differ in sign for some  $x_i$ , then the above discretization treats  $f_{x,i} = 0$ .

For the examples shown below, we use a uniform mesh size  $\delta x = 0.005$ , and  $\delta t = 0.001$  on the domain  $[0, 1]$ , with  $J = 201$  gridpoints. Refining the mesh and reducing the time step ( $\delta x = 0.001$ ,  $J = 1001$ ,  $\delta t = 10^{-5}$ ) does not produce a significant difference in the results.

## 6.2 Evolution toward steady state solutions

Beginning from arbitrary but smooth initial conditions, a typical solution exhibits two distinct phases in its dynamics. First, the populations quickly

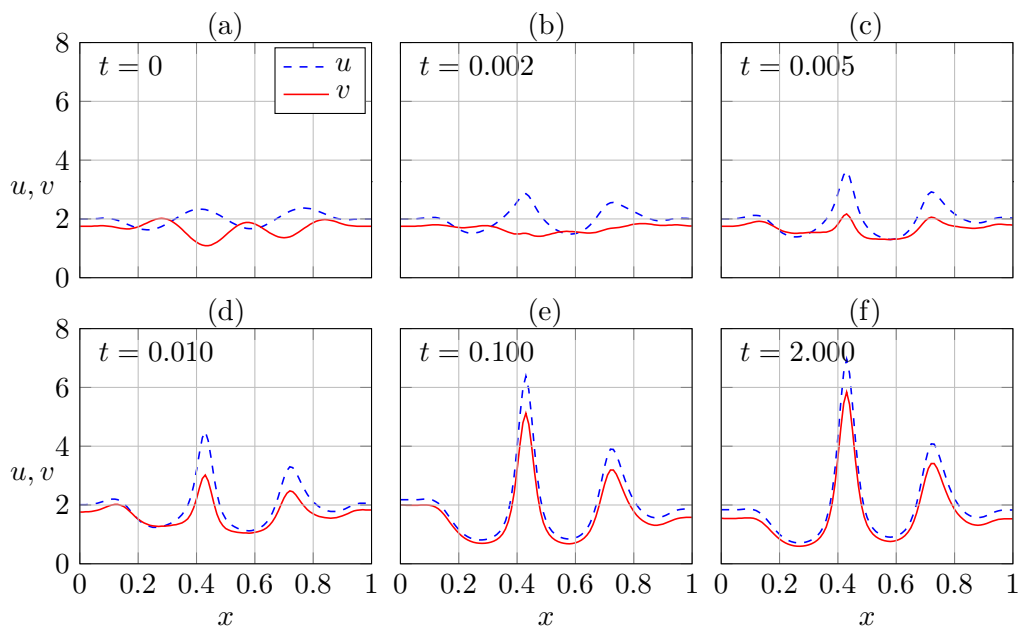


Figure 5: Evolution of a solution to (5.1) toward steady state. The extrema for  $u$  and  $v$  are almost perfectly aligned by the tenth iteration (d),  $t = 0.010$ . The local maxima grow at a decreasing rate as the solution approaches a steady state in (e), where  $u = cv$ . At steady state (f), the fitness function  $f(u, v)$  is constant throughout  $\Omega$ . Solutions shown are for  $\gamma = 0.5$ .

reach a configuration where local extrema of  $u$  and  $v$  are aligned with one another, as well as with the local extrema of the fitness function  $f$ . Once aligned, the local maxima of  $u$  and  $v$  grow while their local minima decrease, but at a decreasing rate as  $\nabla f \rightarrow 0$ , and the solution approaches a steady state.

We can understand this dynamic as follows. Suppose that at time  $t$ ,  $u$  and  $v$  each have a local maximum at a point  $x^* \in \Omega$ . Since  $\nabla u = \nabla v = 0$

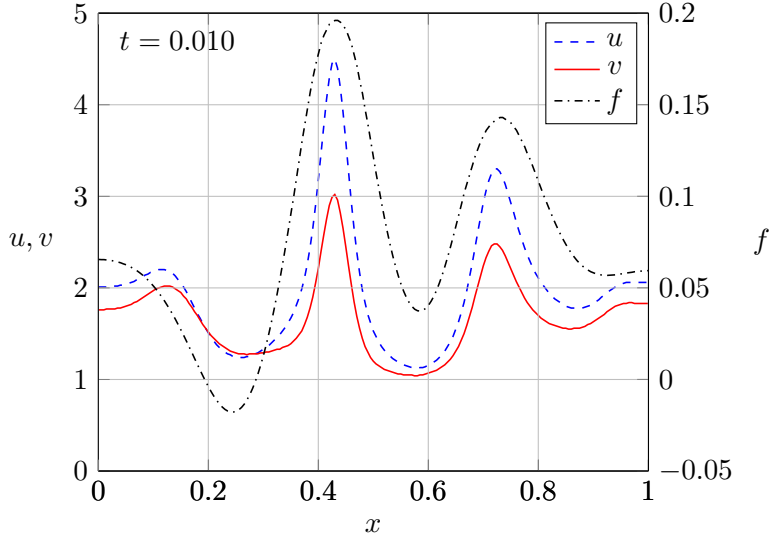


Figure 6: The plot from Figure 5d compared with the fitness  $f(u, v)$ . The extrema of  $u$ ,  $v$ , and  $f$  are nearly aligned. Notice that  $f$  has a different scale than  $u$  and  $v$ . In particular,  $f$  falls below zero over part of the domain.

at the point  $(x^*, t) \in \Omega \times (0, \infty)$ , the solution to (5.1) locally obeys

$$\begin{aligned} u_t(x^*, t) &= -u(x^*, t)\Delta f(x^*, t), \\ v_t(x^*, t) &= -(1 + \gamma)v(x^*, t)\Delta f(x^*, t). \end{aligned}$$

If  $f(\cdot, t)$  also has a local maximum at  $x^*$  and is such that  $\Delta f(x^*, t) \leq \Delta f(x, t)$  for  $x$  in a neighborhood of  $x^*$ , (for example if  $f$  is well approximated by a quadratic in the vicinity of its maximum), then

$$\begin{aligned} u_t(x^*, t) &> u_t(x, t) \geq 0, \\ v_t(x^*, t) &> v_t(x, t) \geq 0, \end{aligned}$$

for  $x$  near  $x^*$ . The rate of increase at  $x^*$  is greater than at nearby points, and the local maxima of  $u$  and  $v$  at  $x^*$  remain at  $x^*$  at a later time  $t + \delta t$ .

Figure 5 demonstrates this typical evolution toward a steady state, with

$\gamma = 0.5$ . The initial conditions are

$$\begin{aligned} u(x, 0) &= 2 + \left( \frac{1}{5} \cos(3\pi x) + \frac{1}{2} \cos(5\pi x) \right) \exp \left( -\frac{(x - \frac{1}{2})^2}{x(1-x)} \right), \\ v(x, 0) &= 1.75 + \left( \frac{3}{10} \cos(2\pi x) + \frac{2}{5} \cos(4\pi x) \right) \exp \left( -\frac{(x - \frac{1}{2})^2}{x(1-x)} \right). \end{aligned} \quad (6.1)$$

The factor  $\exp \left( -\frac{(x - \frac{1}{2})^2}{x(1-x)} \right)$  is included to de-emphasize the role of the boundary, while satisfying the Neumann conditions. Early in the simulation ( $t = 0.010$ , Figure 5d), the local extrema of  $u$  and  $v$  are aligned with one another, and also aligned with the local extrema of the fitness function  $f$  (see Figure 6). Evolution then progresses asymptotically toward a steady state where the fitness  $f$  is constant and  $u(x, t) = cv(x, t)$  throughout the domain  $\Omega$ . During this second phase, the aligned maxima are increasing with time, while the aligned minima are decreasing, but at a decreasing rate as the steady state is approached.

We have observed that for some initial conditions,  $u$  and  $v$  appear to actually reach zero pointwise before the steady state is achieved (in finite time), leading to the development of weak steady state solutions. These initial conditions seem to correlate with  $uv \ll |\nabla f|^2$  in some region of  $\Omega$ . In particular, by decreasing the initial conditions in (6.1) by a constant, we seem to be able to produce a weak steady state solution (see Figure 10). Several examples are included in Section 6.4 below.

### 6.3 Perturbation from Steady State

Figure 7 illustrates the instability of smooth, strictly positive steady states; Figure 7a shows a steady state solution  $(u_s, v_s)$ , where

$$\begin{aligned} u_s &= 1 + \frac{1}{5} \cos(\pi x) + \frac{1}{5} \cos(2\pi x) + \frac{1}{2} \cos(3\pi x) + \frac{1}{100} \cos(5\pi x), \\ v_s &= \frac{9}{10} u_s. \end{aligned} \quad (6.2)$$

This steady state is perturbed at  $t = 0$  (Figure 7b),

$$\begin{aligned} u(x, 0) &= u_s + \frac{1}{100} \cos(4\pi x) + \frac{1}{20} \cos(11\pi x), \\ v(x, 0) &= v_s + \frac{1}{100} \cos(2\pi x) + \frac{1}{20} \cos(7\pi x). \end{aligned} \quad (6.3)$$

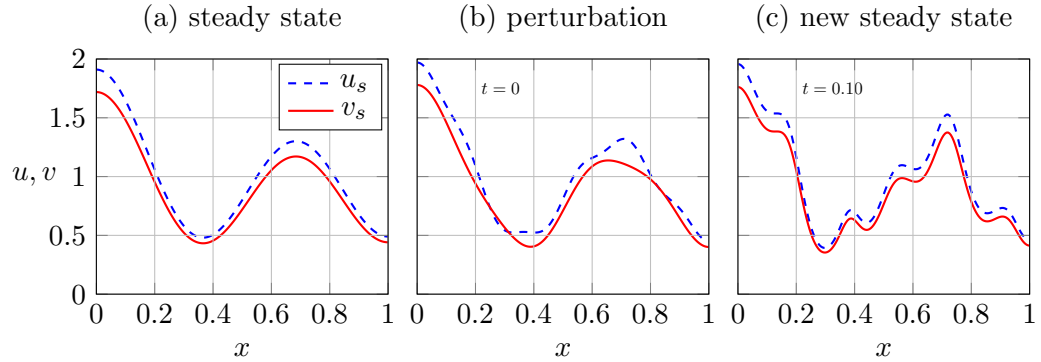


Figure 7: (a) A steady state solution  $(u_s, v_s)$  given by (6.2); (b) perturbation of  $(u_s, v_s)$  given by (6.3); (c) Evolution of perturbed problem to nearby steady state  $(u'_s, v'_s)$ .

With this perturbation as the initial condition, the solution to (5.1) evolves to a nearby steady state,  $(u'_s, v'_s)$ , shown in Figure 7(c).

In Figure 8 we show a simulation for the linearization around a steady state  $(u_s, v_s)$ , where

$$v_s(x) = \cos(2x) \exp(-(\pi - x)^2) + 2, \quad \text{and} \quad u_s(x) = 2v_s(x).$$

This steady-state  $(u_s, v_s)$  is shown by the dashed plots in the figure. The solid blue and black plots show the initial conditions for a perturbation  $\mathbf{w}(x, 0) = (w_1(x, 0), w_2(x, 0))$ , given by

$$w_1(x, 0) = 0.5 \cos(x) - 0.75 \cos(4.5x), \quad w_2(x, 0) = 0.5 \cos(1.5x) + 0.3 \cos(2.5x).$$

Computing the decomposition  $\mathbf{w}(x, t) = c_0(x)\mathbf{e}_0 + c_1(x, t)\mathbf{e}_1$ , we simulate a solution to the linearization (5.10) using the initial condition  $c_1(x, 0)$ . The plot for the final time (a steady state for the linearization) is also shown (the green and orange plots in the figure).

$$w_1(x, T) = u_s(x) + \frac{c}{1 + \gamma} c_0(x) + c_1(x, T), \quad w_2(x, T) = v_s(x) + c_0(x) + c_1(x, T).$$

#### 6.4 Evolution toward weak steady state solutions

As noted in Section 5.1, given certain initial conditions, a solution of (5.1) may evolve to a weak steady state solution. These solutions are continuous

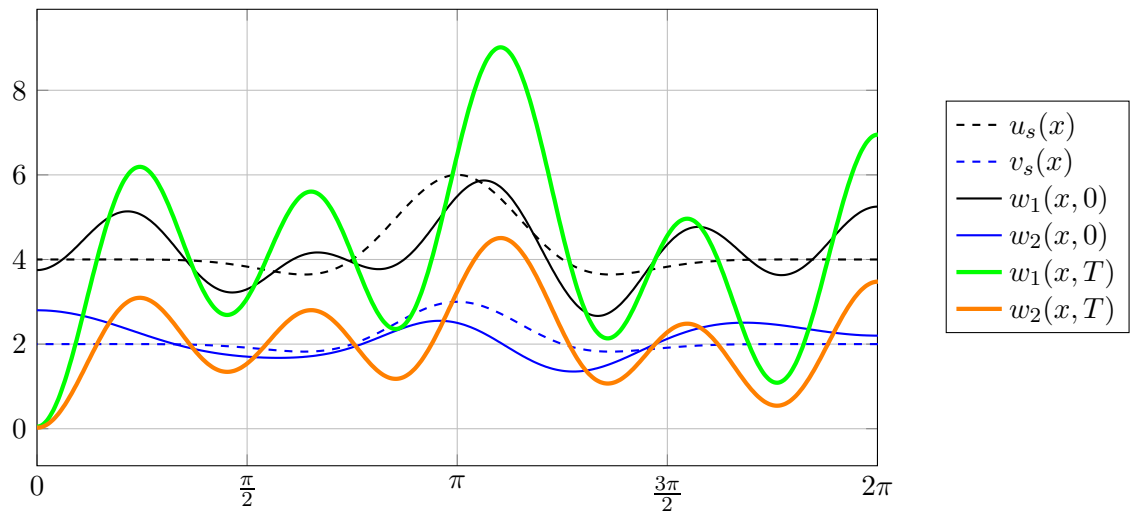


Figure 8: The dashed plots depict a steady state solution  $(u_s, v_s)$ , where  $u_s(x) = 2v_s(x)$ . The functions  $w_1(x, 0)$  and  $w_2(x, 0)$  denote a perturbation of this steady state, which evolves according to the linearization given by (5.8). The functions  $w_1(x, T)$  and  $w_2(x, T)$  denote the steady-state that this perturbation evolves to.

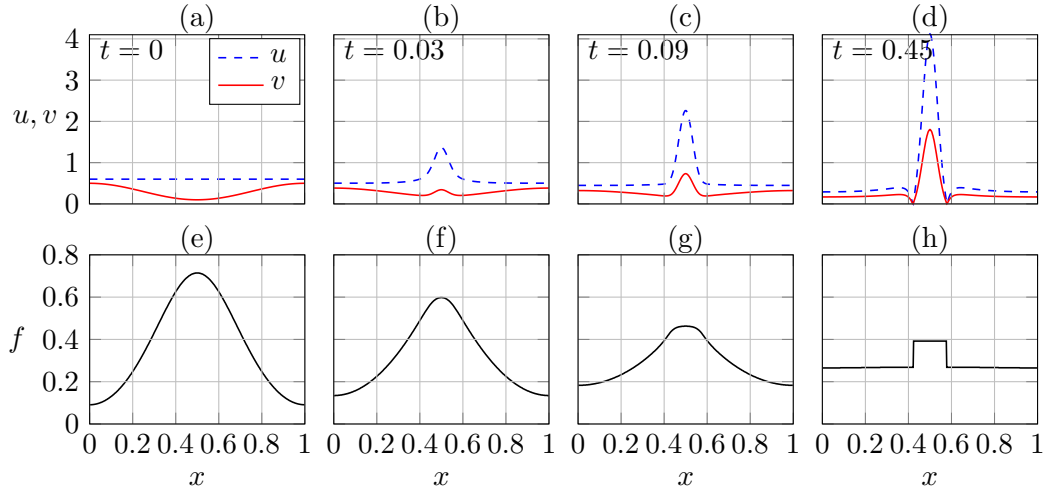


Figure 9: Evolution toward non-smooth steady-state (Example 1). The fitness  $f$  approaches a piecewise constant function.

but not smooth, and the corresponding fitness function  $f$  becomes piecewise constant in the steady state. We present several numerical examples.

It will be helpful to first discuss the implicit dynamics of  $f$ , the fitness function for  $u$ . Recall from Section 2 that  $f$  depends only on  $u$  and  $v$ ,

$$f(u, v) = \frac{a_{11}u + a_{12}v}{(u, v)},$$

where we have assumed that  $a_{11} - a_{12} = 1$ . We will use the notation  $f(x, t)$  to refer to  $f(u(x, t), v(x, t))$ . Given a solution  $(u, v)$  to (5.1), notice that

$$f_t = \frac{1}{(u+v)^2}(vu_t - uv_t), \quad (6.4)$$

from which we can obtain

$$f_t = \frac{1}{(u+v)^2} \left[ \gamma uv \Delta f - |\nabla f|^2 + \gamma u \nabla v \cdot \nabla f \right]. \quad (6.5)$$

If  $u$  and  $v$  are smooth strictly positive solutions, then the coefficient on  $\Delta f$  in (6.5) is positive, and it is clear from the maximum principle that  $f$  attains its maximum and minimum values on the parabolic boundary,  $\partial\Omega \times [t = 0]$ .

**Weak solution - Example 1.** Let  $(u(x, t), v(x, t))$  be a weak solution to (5.1), with the initial conditions

$$u(x, 0) = \frac{3}{5}, \quad v(x, 0) = \frac{1}{5} \cos(2\pi x) + \frac{3}{10}. \quad (6.6)$$

In Figure 9, the top row depicts the evolution of  $u(x, t)$  and  $v(x, t)$  (Fig. 9a-d), while the bottom row depicts  $f$ , the fitness of population  $u$  (Fig. 9e-h). The initial conditions were chosen so that the fitness  $f$  would have a single peak and no interior minima, and such that  $v(x, 0)$  is nearly zero over part of the domain. Notice in Figure 9c and g that the local minima of  $u$  and  $v$  are nearly aligned. In the vicinity of these local minima we have the following conditions

1.  $f_{xx} > 0$ ,
2.  $|\nabla f|^2 > 1$ ,
3. the product  $uv \ll 1$ .

If  $u(\cdot, t)$  has a local minimum at  $x^*$ , then at the point  $(x^*, t)$  we have

$$u_t(x^*, t) = -u(x^*, t)\Delta f(x^*, t). \quad (6.7)$$

From the convexity of  $f$ , it is clear that  $u$  and  $v$  are decreasing in the vicinity of the local minima. If also,  $|\nabla f|^2 > \gamma uv \Delta f$ , then we see from (6.5) that  $f$  will also be decreasing. As a result, in the vicinity of the local minima of  $u$  and  $v$ , both  $\Delta f$  and  $|\nabla f|$  are increasing. Notice how this differs from the case where local minima of  $u$  and  $v$  are aligned with a local minimum of  $f$ . We have

$$\Delta f = \frac{v\Delta u - u\Delta v}{(u+v)^3} > 0,$$

with  $\Delta u$  and  $\Delta v$  increasing. Therefore

$$\Delta f \sim \frac{u\Delta v}{v^3},$$

If we assume that  $\Delta v$  is not decreasing and that  $u \sim v$ , we conclude that  $\Delta f \sim u^{-2}$  in the vicinity of  $x^*$ .

As long as the local minimum for  $u$  remains at  $x^*$  as  $t$  increases, then

$$u_t(x^*, t) = -u(x^*, t)\Delta f(x^*, t) \sim -u^{-1}(x^*, t)$$

Thus we expect  $u \sim \sqrt{C-t}$  for some constant  $C > 0$ , which implies  $u(x^*, t)$  goes to zero in finite time.

The dynamic here is one in which both  $u$  and  $v$  locally sense a high fitness gradient, and their response has the effect of increasing this gradient, thus accelerating the rate at which the densities  $u$  and  $v$  locally approach zero.

**Weak solution - Example 2.** In our second example, we modify the initial conditions (6.1) from the example in Section 6.2, subtracting the constant 1 from each initial condition (see Figure 10(a),(b)). This changes the relative values of  $u$  and  $v$ , thus altering the fitness profile and setting up the condition,  $uv \ll 1$  on part of the domain, that leads to weak solutions (Figure 10(c),(d)). In the steady state (Figure 10(e),(f)), the fitness profile for the modified problem is piecewise constant.

**Weak solution - Example 3.** Our third weak solution is shown in Figure 11, with initial conditions

$$\begin{aligned} u(x, 0) &= \frac{3}{5}, \\ v(x, 0) &= \frac{2}{5} + \left(\frac{2}{5} \cos(5\pi x)\right) \exp\left(-\frac{(x - \frac{1}{2})^2}{x(1-x)}\right). \end{aligned} \tag{6.8}$$

Notice from Figure 11(a),(d) that at time  $t = 0$ , the local minima of  $v$  correspond to local maxima of  $f$ , at the points  $x^*$  and  $y^*$  in the figure. The local maxima of  $f$  drive aggregation of  $u$  and  $v$  in the vicinity of  $x^*$  and  $y^*$  (Figure 11(b)), which in turn leads to local minima in  $u$  and  $v$  near  $x^*$  and  $y^*$ , with large gradients in  $f$ , the conditions that drive  $u$  and  $v$  to zero.

## 6.5 A spatial Lotka–Volterra model

In our final example, we use the fitness gradient flux to construct a spatial Lotka–Volterra model. The non-spatial model has a stable steady state, which we show here to be destabilized by cross-diffusion when the fitness gradient flux is included. Our approach will be discussed more fully in a future paper.

Consider a generalized Lotka–Volterra ODE model

$$\begin{aligned}\dot{u} &= g_1(u, v) = u(c_1 - c_2u - c_3v), \\ \dot{v} &= g_2(u, v) = v(k_1 + k_2u - k_3v),\end{aligned}\tag{6.9}$$

where  $u$  and  $v$  are densities of the two species subject to logistic growth, and the constants  $c_i, k_i > 0$ . The growth rate of  $v$  is enhanced by  $u$ , while the growth rate of  $u$  is decreased by  $v$ , as might occur in a predator-prey or host-parasite type interaction, where  $u$  is the prey and  $v$  is the predator. We note however that in the standard Lotka–Volterra predator-prey system, the constant  $k_1$  would be strictly negative. If the null-clines  $c_1 = c_2u - c_3v$  and  $k_1 = -k_2u + k_3v$  in the  $(u, v)$ -phase plane intersect in the interior of the first quadrant, then (6.9) has a stable steady state  $(u^*, v^*)$ , with  $u^*, v^* > 0$ .

Linearizing (6.9) around the steady state and letting

$$J_{(u^*, v^*)} = \begin{bmatrix} \partial_u g_1 & \partial_v g_1 \\ \partial_u g_2 & \partial_v g_2 \end{bmatrix}_{(u^*, v^*)} = \begin{bmatrix} -k_2u^* & -k_3u^* \\ c_2v^* & -c_3v^* \end{bmatrix},$$

we see that  $J$  has the following sign structure:

$$\begin{bmatrix} - & - \\ + & - \end{bmatrix}.\tag{6.10}$$

Since  $\partial_u g_1$  and  $\partial_v g_2$  have the same sign at the steady state, the ODE system does not display an activator-inhibitor dynamic, and the steady state cannot be destabilized by diffusion [28]. However, a cross-diffusive instability occurs when we spatially extend this model as a fitness gradient flux system

$$\begin{aligned}\partial_t u &= -\nabla \cdot (u \nabla f) + u(c_1 - c_2u - c_3v), \\ \partial_t v &= -(1 + \gamma) \nabla \cdot (v \nabla g) + v(k_1 + k_2u - k_3v),\end{aligned}\tag{6.11}$$

where the fitness  $f$  is as defined in Section 2 above, and satisfies the same conditions as assumed in our previous analysis. The instability is illustrated with a numerical example in Figure 12. Note that an individual in either the prey or predator population benefits by locating itself where there is a high density of prey relative to predators. Prey tend to aggregate, and predators follow. The result is an alignment dynamic for the extrema as shown in Figure 12, very similar to the fitness gradient flux system discussed previously. Spatial variation of the ratio  $u/v$  in the initial conditions give

rise to local aggregations, as the populations align in a spatially structured steady state. Unlike Turing patterns, however, there is no characteristic wavelength; steady state patterns depend on initial conditions.

## 7 Conclusions

Our results show that under a fitness-based dispersal mechanism where the fitness has some dependence on individual interactions, as in an evolutionary game, variations in the ratio of population densities lead to spatial structure as populations ascend local fitness gradients.

The interaction between populations in our model has a predator-prey or cooperative-exploitative dynamic, as in the standard prisoner's dilemma and hawk-dove games. Individuals of both populations benefit by locating themselves where the density of the cooperative or prey species  $u$  is large, relative to the density of the exploitative or predatory species  $v$ .

We can consider interesting extensions of the model by coupling this fitness gradient flux with ODE systems for relevant local population dynamics, as we have done in the spatial Lotka–Volterra model in Section 6.5. We also expect this spatial coupling to have relevance to public-goods interactions that describe coexistence of cooperative and exploitative behavior as has been observed, for example, in polymorphic populations of yeast [20].

Although here we have focused on directed motion in a non-diffusive limit, it is natural to consider including a component of diffusion and/or a law of motion for each population in the absence of the other, as well as a density dependent fitness or term describing interactions when  $u + v$  is small and the mean-field assumptions of evolutionary game theory should not be expected to hold. We also have not included in our basic model any term that *a priori* prevents unlimited aggregation. The higher sensitivity of population  $v$ , to the fitness gradient ( $\gamma > 0$  in (5.1)) allows the exploitative population to in some sense overtake  $u$  and limit its aggregation. We expect that if the cooperative population  $u$  has the higher sensitivity that blow up would occur, although this remains to be shown.

It is also interesting to consider non-transitive (cyclic) games for three players, such as the classic Rock, Paper, Scissors game. Through numerical simulations, we have shown the development of spiral waves in 2D in a previous paper, and we suspect that such models also have periodic solutions

when coupled with particular local population dynamics [15].

**Acknowledgements:** We would like to thank H. K. Jenssen and Y. Lou for helpful discussions, and C. Cosner and T. Reluga for comments. AB was supported by NSF Grant CMMI-1463482.

## References

- [1] Herbert Amann. Dynamic theory of quasilinear parabolic equations I. Abstract evolution equations. *Nonlinear Analysis: Theory, Methods & Applications*, 12(9):895–919, September 1988. doi:10.1016/0362-546X(88)90073-9.
- [2] Herbert Amann. Dynamic Theory of Quasilinear Parabolic Systems: III. Global Existence. *Math. Z.*, 202:219–250, 1989. doi:10.1007/BF02571246.
- [3] Herbert Amann. Dynamic Theory of Quasilinear Parabolic Equations II. Reaction-Diffusion Systems. *Differential and Integral Equations*, 3(1):13–75, 1990. URL <https://projecteuclid.org/euclid.die/1371586185>.
- [4] D. G. Aronson. The role of diffusion in mathematical population biology: Skellam revisited. In *Mathematics in biology and medicine (Bari, 1983)*, volume 57 of *Lecture Notes in Biomath.*, pages 2–6. Springer, Berlin, 1985. doi:10.1007/978-3-642-93287-8\_1.
- [5] N. Bacaër. *A Short History of Mathematical Population Dynamics*. Springer, 2011. doi:10.1007/978-0-85729-115-8.
- [6] Jacob Bedrossian, Nancy Rodríguez, and Andrea L. Bertozzi. Local and global well-posedness for aggregation equations and Patlak-Keller-Segel models with degenerate diffusion. *Nonlinearity*, 24:1683–1714, 2011. doi:10.1088/0951-7715/24/6/001.
- [7] Andrea L. Bertozzi and Dejan Slepcev. Existence and Uniqueness of Solutions to an Aggregation Equation with Degenerate Diffusion. *Communications on Pure and Applied Analysis*, 9(6):1617–1637, 2010. doi:10.3934/cpaa.2010.9.1617.

- [8] Robert Stephen Cantrell and Chris Cosner. *Spatial ecology via reaction-diffusion equations*. Wiley Series in Mathematical and Computational Biology. John Wiley & Sons, Ltd., Chichester, 2003. ISBN 0-471-49301-5. doi:10.1002/0470871296.
- [9] Robert Stephen Cantrell, Chris Cosner, and Yuan Lou. Approximating the ideal free distribution via reaction-diffusion-advection equations. *J. Differential Equations*, 245(12):3687–3703, 2008. doi:10.1016/j.jde.2008.07.024.
- [10] Robert Stephen Cantrell, Chris Cosner, Yuan Lou, and Chao Xie. Random dispersal versus fitness-dependent dispersal. *J. Differential Equations*, 254(7):2905–2941, 2013. doi:10.1016/j.jde.2013.01.012.
- [11] S. Childress and J. K. Percus. Nonlinear aspects of chemotaxis. *Mathematical Biosciences*, 56(4):217–237, 1981. doi:10.1016/0025-5564(81)90055-9.
- [12] Chris Cosner. A dynamic model for the ideal-free distribution as a partial differential equation. *Theoretical Population Biology*, 67(2):101–108, 2005. doi:10.1016/j.tpb.2004.09.002.
- [13] Chris Cosner. Reaction-diffusion-advection models for the effects and evolution of dispersal. *Discrete Contin. Dyn. Syst.*, 34(5):1701–1745, 2014. doi:10.3934/dcds.2014.34.1701.
- [14] Ross Cressman and Vlastimil Kivan. Migration dynamics for the ideal free distribution. *The American Naturalist*, 168(3):pp. 384–397, 2006. doi:10.1086/506970.
- [15] Russ DeForest and Andrew Belmonte. Spatial pattern dynamics due to the fitness gradient flux in evolutionary games. *Physical Review E*, 87(6):062138, June 2013. doi:10.1103/PhysRevE.87.062138.
- [16] Lloyd Demetrius and Volker Matthais Gundlach. Game theory and evolution: finite size and absolute fitness measures. *Mathematical Biosciences*, 168:9–38, 2000. doi:10.1016/S0025-5564(00)00042-0.
- [17] David Easley and Jon Kleinberg. *Networks, Crowds, and Markets: Reasoning about a Highly Connected World*. Cambridge University

Press, 2010. URL

<http://www.cs.cornell.edu/home/kleinberg/networks-book>.

- [18] R. A. Fisher. The wave of advance of advantageous genes. *Annals of Eugenics*, 7(4):355–369, 1937. doi:10.1111/j.1469-1809.1937.tb02153.x.
- [19] Stephen D. Fretwell and Henry L. Lucas Jr. On territorial behavior and other factors influencing habitat distribuion in birds. I. Theoretical development. *Acta Biotheoretica*, 14:16–36, 1970. ISSN 0001-5342. doi:10.1007/BF01601953.
- [20] Duncan Greig and Michael Travisano. The prisoner’s dilemma and polymorphism in yeast SUC genes. *Proceedings of the Royal Society of London B: Biological Sciences*, 271(Suppl 3):S25–S26, 2004. ISSN 0962-8452. doi:10.1098/rsbl.2003.0083.
- [21] W. D. Hamilton. Geometry for the Selfish Herd. *J. theor. Biol.*, 31: 295–311, 1971. doi:10.1016/0022-5193(71)90189-5.
- [22] J. Hofbauer and K. Sigmund. *Evolutionary Games and Population Dynamics*. Cambridge University Press, 1998. ISBN 9780521625708.
- [23] Dirk Horstmann. From 1970 until present: the Keller-Segel model in chemotaxis and its consequences, 2003. URL [http://www.mis.mpg.de/preprints/2003/preprint2003\\_3.pdf](http://www.mis.mpg.de/preprints/2003/preprint2003_3.pdf). Preprint.
- [24] Thomas Laurent. Local and Global Existence for an Aggregation Equation. *Communications in Partial Differential Equations*, 32: 1941–1964, 2007. doi:10.1080/03605300701318955.
- [25] S. H. Lui. *Numerical Analysis of Partial Differential Equations*. John Wiley & Sons, 2011. ISBN 978-1-118-11113-0.
- [26] M. Morisita. Measuring of habitat value by environmental density method. In GP Patil, EC Pielou, and WE Waters, editors, *Statistical Ecology Vol. I*, pages 379–401. The Pennsylvania State University Press, 1971.
- [27] Lesley J. Morrell and Richard James. Mechanisms for aggregation in animals: rule success depends on ecological variables. *Behavioral Ecology*, 19(1):193–201, 2008. doi:10.1093/beheco/arm122.

- [28] J. D. Murray. *Mathematical biology. I*, volume 17 of *Interdisciplinary Applied Mathematics*. Springer-Verlag, New York, third edition, 2002. ISBN 0-387-95223-3. An introduction.
- [29] Akira Okubo. Dynamical aspects of animal grouping: Swarms, schools, flocks, and herds. *Advances in Biophysics*, 22:1–94, 1986. doi:10.1016/0065-227X(86)90003-1.
- [30] Akira Okubo and Simon A. Levin. *Diffusion and ecological problems: modern perspectives*, volume 14 of *Interdisciplinary Applied Mathematics*. Springer-Verlag, New York, second edition, 2001. ISBN 0-387-98676-6. doi:10.1007/978-1-4757-4978-6.
- [31] Julia T. Parrish, Steven V. Viscido, and Daniel Grünbaum. Self-Organized Fish Schools: An Examination of Emergent Properties. *Biological Bulletin*, 202(3):296–305, 2002. doi:10.2307/1543482.
- [32] Michael L. Rosenzweig and Zvika Abramsky. Detecting density-dependent habitat selection. *The American Naturalist*, 126(3): pp. 405–417, 1985. URL <http://www.jstor.org/stable/2461364>.
- [33] Jonathan T. Rowell. Tactical population movements and distributions for ideally motivated competitors. *The American Naturalist*, 176(5): pp. 638–650, 2010. doi:10.1086/656494.
- [34] Graeme D. Ruxton and Thomas N. Sherratt. Aggregation, defence and warning signals: The evolutionary relationship. *Proceedings: Biological Sciences*, 273(1600):pp. 2417–2424, 2006. URL <http://www.jstor.org/stable/25223621>.
- [35] N. Shigesada, K. Kawasaki, and E. Teramoto. Spatial segregation of interacting species. *Journal of theoretical biology*, 79(1):83–99, July 1979. doi:10.1016/0022-5193(79)90258-3.
- [36] J. G. Skellam. The formulation and interpretation of mathematical models of diffusional processes in population biology. In M. S. Bartlett and R. W. Hiorns, editors, *The Mathematical Theory of the Dynamics of Biological Populations*, pages 63–85. Academic Press, London, 1973.

- [37] J.G. Skellam. Random Dispersal in Theoretical Populations. *Bulletin of Mathematical Biology*, pages 135–165, 1991. doi:10.1007/BF02464427. Reprinted from *Biometrika*, **38**, 1951.
- [38] Peter D. Taylor and Leo B. Jonker. Evolutionarily stable strategies and game dynamics. *Math. Biosci.*, 40(1-2):145–156, 1978. doi:10.1016/0025-5564(78)90077-9.
- [39] G. T. Vickers. Spatial patterns and ESS's. *J. Theoret. Biol.*, 140(1): 129–135, 1989. doi:10.1016/S0022-5193(89)80033-5.
- [40] Frederick J. Wrona and R. W. Jamieson Dixon. Group size and predation risk: A field analysis of encounter and dilution effects. *The American Naturalist*, 137(2):pp. 186–201, 1991. URL <http://www.jstor.org/stable/2462112>.
- [41] Qiuju Xu, Andrew Belmonte, Russ deForest, Chun Liu, and Zhong Tan. Strong solutions and instability for the fitness gradient system in evolution games between two populations. *Journal of Differential Equations*, 262:4021–4051, 2017. doi:10.1016/j.jde.2016.12.008.

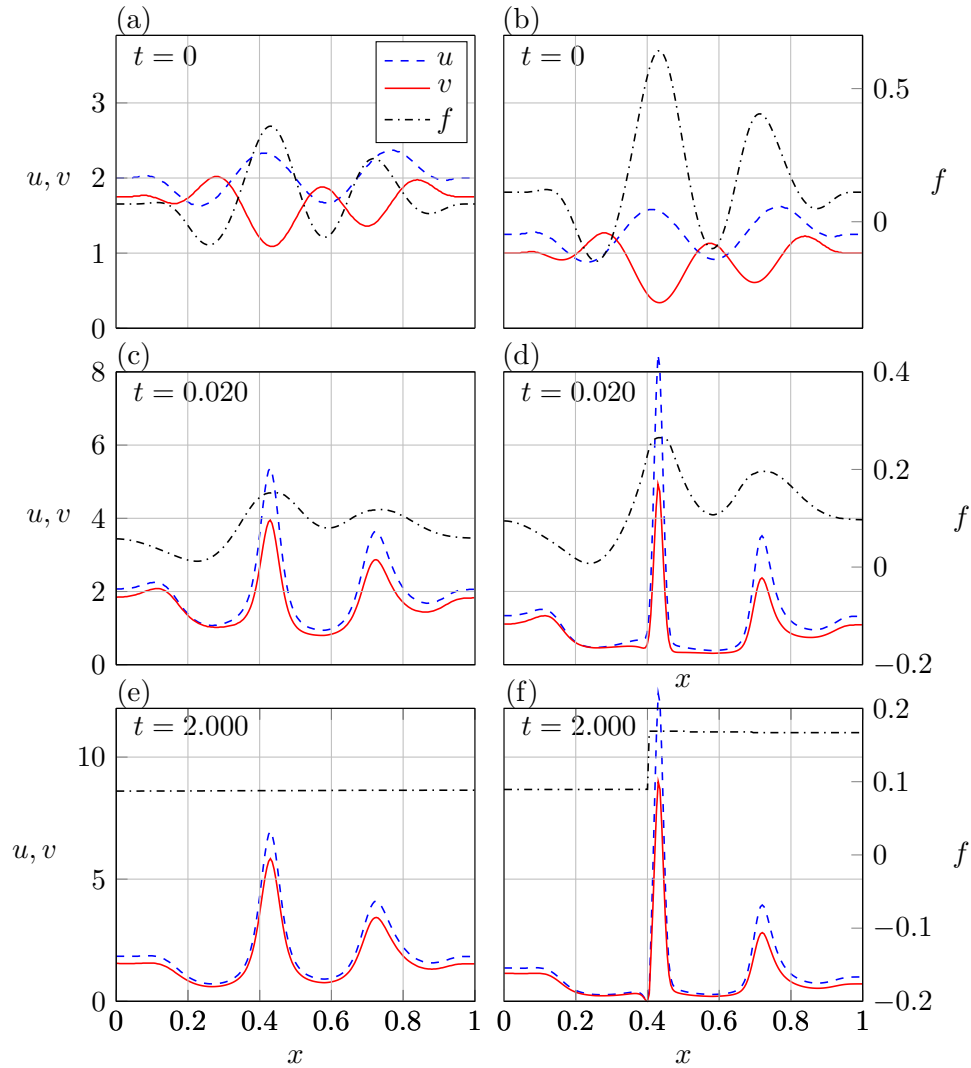


Figure 10: Comparison for two solutions whose initial conditions differ by a constant. In each plot scaling for densities  $u$  and  $v$ , is indicated on the left, while scaling for  $f(u, v)$  is indicated on the right. Left column shows evolution for (a) initial conditions  $u_0, v_0$  from (6.1). The right column shows evolution for (b) initial conditions are  $u_0 - \frac{3}{4}, v_0 - \frac{3}{4}$ . This produces large gradients in the fitness, along with regions where the product  $uv \ll 1$  leading to a weak solution (see text).

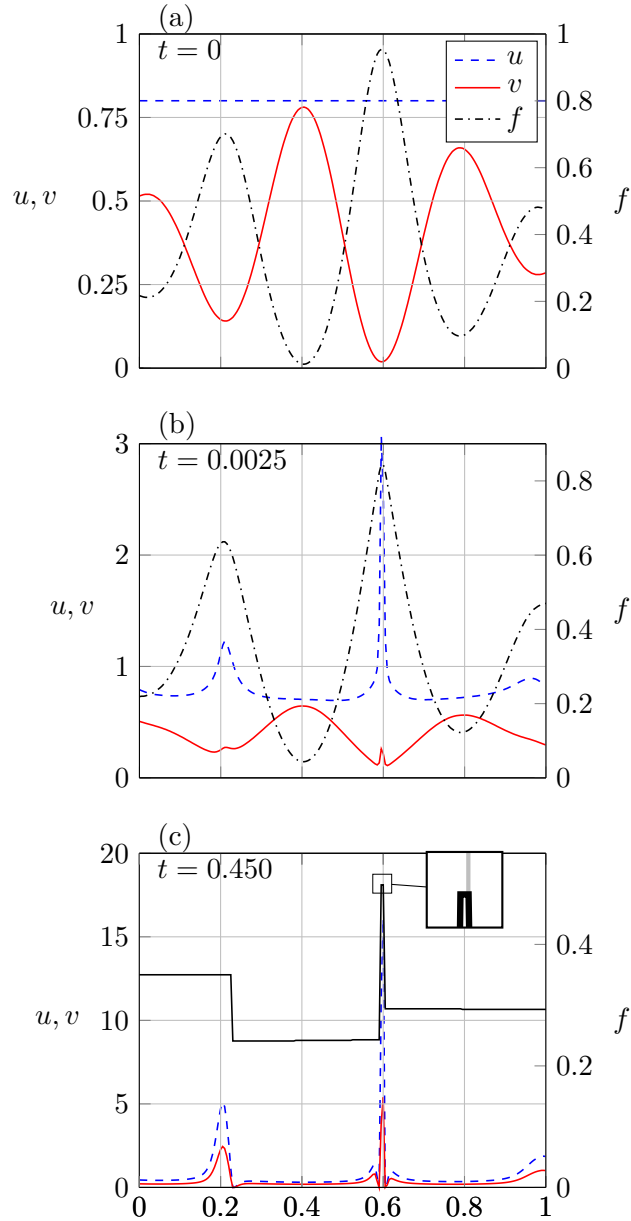


Figure 11: Example 3: (a) initial conditions that produce large gradients in the fitness and regions where  $uv \ll 1$  (near  $x = 0.6$ ), leading to a weak steady state solution with a fitness that is piecewise constant in the steady state (c). Note that the fitness is constant on a small interval around  $x = 0.6$  (see inset).

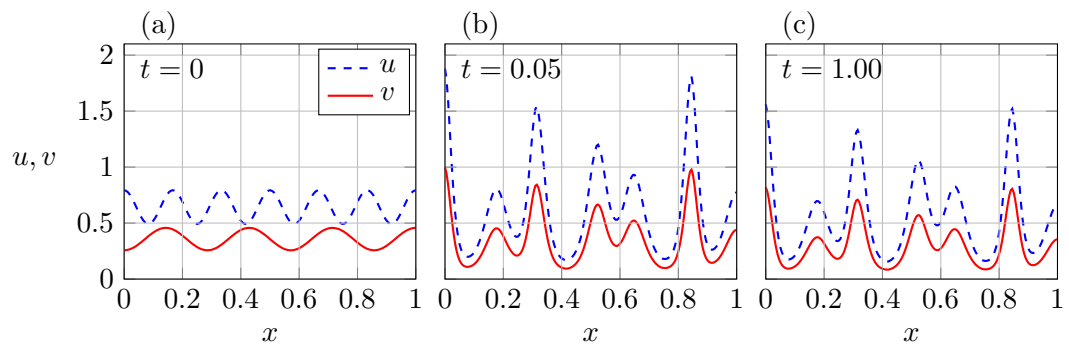


Figure 12: Spatially-extended Lotka–Volterra model (6.11), with  $k_1 = k_2 = k_3 = 1$ ,  $c_1 = 3/2$ ,  $c_2 = 1$ ,  $c_3 = 6$ .